

SELECTION OF POTENTIAL MINERAL DEPOSITS IN
SOUTHWESTERN SINAI USING LANDSAT IMAGERY

By

KENNETH ELMUS QUINN

Bachelor of Science
University of Alabama
Tuscaloosa, Alabama
1970

Master of Library Science
University of Alabama
Tuscaloosa, Alabama
1974

Submitted to the Faculty of the Graduate College
of the Oklahoma State University
in partial fulfillment of the requirements
for the Degree of
MASTER OF SCIENCE
July, 1983



SELECTION OF POTENTIAL MINERAL DEPOSITS IN
SOUTHWESTERN SINAI USING LANDSAT IMAGERY

Thesis Approved:

Douglas C. Kent

Thesis Adviser

Atkinson

Zuhair al-Shaikh

Wayne A. Pettyjohn

Navel Danar

Norman D. Durbin

Dean of the Graduate College

ACKNOWLEDGMENTS

A number of people in two countries have aided me on this project. In Egypt, Dr. M. A. Abdel Hady, the Head of the Remote Sensing Center was of immense help. Special thanks go to Dr. E. M. El Shazly, Dr. M. M. El Shazly, and Dr. Raafat Misak. The entire staff of the Remote Sensing Center in Cairo was most helpful and cooperative.

At Oklahoma State University, I wish to thank Dr. J. V. Parcher, Head of the School of Civil Engineering. The staff of the Oklahoma State University Center for Applications of Remote Sensing under the direction of Dr. Steven Walsh provided digital processing services. In the Geology Department, I wish to thank Dr. Wayne Pettyjohn, Dr. Zuhair Al-Shaieb and Dr. Arthur Hounslow for comments on certain sections of the study.

I wish to thank Kevin Horstman of Cities Service Company for providing some photographic images of Sinai.

Special thanks to Dr. Abdel Hady, the Egyptian Remote Sensing Center, and the United Nations Environmental Fund for providing the LANDSAT imagery and for making possible the collection of ground truth in Sinai.

Dr. Douglas Kent, my major adviser, is due my gratitude for suggesting the research, arranging funding, and guiding the research.

Finally, I most gratefully acknowledge the encouragement, patience and work that I received from my wife, Cynthia Dausman Quinn.

TABLE OF CONTENTS

| Chapter | Page |
|---|------|
| I. PURPOSE OF STUDY. | 1 |
| II. OVERVIEW OF STUDY AREA. | 2 |
| III. PREVIOUS INVESTIGATIONS | 5 |
| A. Geology of Sinai | 5 |
| B. Landsat Methods. | 6 |
| IV. GEOLOGY | 13 |
| A. Geologic History of Southern Sinai | 13 |
| B. Lineaments and Their Relationship to Tectonics | 26 |
| C. Hydrogeology | 30 |
| D. Known Copper Deposits and Mines in Sinai | 31 |
| E. Description of Copper Deposits Examined in the Field. | 34 |
| El Tarr | 34 |
| Regeita Locality. | 41 |
| F. Ore Deposition | 47 |
| V. USE OF REMOTE SENSING TECHNIQUES. | 50 |
| A. Background | 50 |
| B. Computer Processing of the Scene | 51 |
| C. Photographic Techniques. | 65 |
| VI. CONCLUSIONS | 66 |
| VII. RECOMMENDATIONS | 68 |
| BIBLIOGRAPHY. | 69 |
| APPENDIX A - LINEAMENT MAPS | 72 |
| APPENDIX B - BAND RATIO CLASSIFICATION PLOTS OF SELECTED AREAS. | 80 |
| APPENDIX C - EXCERPTS FROM ROAD LOG | 90 |
| APPENDIX D - EXPLORATION TARGET LOCATIONS | 95 |

LIST OF TABLES

| Table | Page |
|---|------|
| I. Reflectance Value Means for Band Ratio Data. | 57 |
| II. Frequency of Classes Within the Target Areas | 58 |
| III. Frequency Counts - Classes of Band Ratioed Scene | 59 |
| IV. Target Characterization. | 60 |
| V. Pixel Class Frequency in Target Areas. | 62 |

LIST OF FIGURES

| Figure | Page |
|---|------|
| 1. Landsat Image 1109-07493 (Not All of Image Shown). Image Provided by Cities Service Co. | 3 |
| 2. Reflectance Spectra of Various Igneous Rocks (Top and Middle) and of Alteration Minerals (Bottom) From Rowan et al., 1976. | 9 |
| 3. Generalized Precambrian Stratigraphy of the Sinai Peninsula Modified From Shimron, 1980 | 14 |
| 4. Index Map, Geological and Lineament Map Sectors. | 15 |
| 5. List of Symbols, Figures 6-12. | 16 |
| 6. Geologic Map of Southern Sinai Precambrian, Sector 1 (See Figure 5 for Legend) | 17 |
| 7. Geologic Map of Southern Sinai Precambrian, Sector 2 (See Figure 5 for Legend) | 18 |
| 8. Geologic Map of Southern Sinai Precambrian, Sector 3 (See Figure 5 for Legend) | 19 |
| 9. Geologic Map of Southern Sinai Precambrian, Sector 4 (See Figure 5 for Legend) | 20 |
| 10. Geologic Map of Southern Sinai Precambrian, Sector 5 (See Figure 5 for Legend) | 21 |
| 11. Geologic Map of Southern Sinai Precambrian, Sector 6 (See Figure 5 for Legend) | 22 |
| 12. Geologic Map of Southern Sinai Precambrian, Sector 7 (See Figure 5 for Legend) | 23 |
| 13. Plate Tectonics in the Sinai Region (From Robson 1971) . . | 27 |
| 14. Lineament Directions in Study Area | 28 |
| 15. Aphanitic Dike at El Tarr. | 35 |
| 16. Granite Intrusion at El Tarr. Gr = Granite, S = Schist. . | 36 |

| Figure | Page |
|---|------|
| 17. Wadi at El Tarr. | 37 |
| 18. Hill Opposite El Tarr Deposit. F = Fault, D = Aphanitic Dike | 38 |
| 19. Photomicrograph of Thin Section T-3 Under Cross Nicols . . | 40 |
| 20. Regeita Mine, Looking North. F = Fault, D = Dike. | 42 |
| 21. Photomicrograph of Thin Section of SK-11, Showing Serici- tization of Plagioclase. Cross Nicols. P = Plagio- clase, S = Sericite. | 44 |
| 22. Photomicrograph of Thin Section of R-3, Under Cross Nicols, Showing Chrysocolla (?) Lining a Vug. Q = Quartz, C = Chrysocolla. | 45 |
| 23. Conceptual Model of Ore Deposition | 49 |
| 24. Geological Data Flow Chart | 52 |
| 25. Computer Data Flow Chart | 53 |
| 26. Lineament Map, Sector 1 (See Figure 4 for Index) | 73 |
| 27. Lineament Map, Sector 2 (See Figure 5 for Index) | 74 |
| 28. Lineament Map, Sector 3 (See Figure 5 for Index) | 75 |
| 29. Lineament Map, Sector 4 (See Figure 5 for Index) | 76 |
| 30. Lineament Map, Sector 5 (See Figure 5 for Index) | 77 |
| 31. Lineament Map, Sector 6 (See Figure 5 for Index) | 78 |
| 32. Lineament Map, Sector 7 (See Figure 5 for Index) | 79 |
| 33. Symbols Used for Band Ratio Plots. | 81 |
| 34. Target 19, Band Ratio Classification, File 1, Scale 1:98, 425. | 82 |
| 35. Target 19, Band Ratio Classification, File 2, Scale 1:98, 425. | 83 |
| 36. Target 19, Band Ratio Classification, File 3, Scale 1:98, 425. | 84 |
| 37. Regeita Area, Band Ratio Classification, Band 1, Scale 1:98, 425. | 85 |

| Figure | Page |
|--|------|
| 38. Regeita Area, Band Ratio Classification, Band 2, Scale 1:98, 425. | 86 |
| 39. Regeita Area, Band Ratio Classification, Band 3, Scale 1:98, 425. | 87 |
| 40. Target 19 Plot Showing Closeness of Match to Altered Rock Spectral Reflectance Values, Using Band Ratio Data. Black = 3 Ratios Match, Diagonal = 2 Match, Dot = 1 Match. | 88 |
| 41. Regeita Area Plot Showing Closeness of Match to Altered Rock Spectral Reflectance Values, Using Band Ratio Data. Black = 3 Ratios Match, Diagonal = 2 Match, Dot = 1 Match. | 89 |
| 42. Wadi at Abu Suweira. | 93 |

CHAPTER I

PURPOSE OF STUDY

The purpose of the study was to evaluate an area of the Sinai Peninsula of Egypt for evidence of hydrothermal mineralization, using as principal tools remote sensing methods. The area investigated was the portion of Sinai covered by Landsat image 1109-07493 and underlain by igneous or metamorphic rocks.

This research is part of an ongoing study of desertification and of natural resources in Egypt. It is a cooperative effort involving the National Science Foundation of the United States and the government of Egypt. The study conducted by Oklahoma State University's School of Civil Engineering, School of Electrical Engineering, Department of Geography, and Department of Geology, in cooperation with Egypt's Remote Sensing Center in Cairo, which is headed by Dr. M. A. Abdel Hady, who is also a Professor of Civil Engineering at Oklahoma State University.

CHAPTER II

OVERVIEW OF STUDY AREA

The study area involves igneous and metamorphic rocks of southwestern Sinai, specifically those covered by Landsat image 1109-07493 (path 188, row 40). The coordinates of this image are:

| | | |
|-----------|-------------------------|-------------------------|
| NE corner | 29 ^o 17'58"N | 34 ^o 28'17"E |
| NW corner | 29 ^o 34'59"N | 32 ^o 37'34"E |
| SW corner | 28 ^o 02'53"N | 32 ^o 10'22"E |
| SE corner | 27 ^o 46'12"N | 33 ^o 59'32"E |

The Sinai peninsula is an extreme desert; rainfall averages 50 mm a year in the southern half. The wet season is December through April and may include snowfall on the higher peaks. The temperature range is from a few degrees below 0^o Centigrade to approximately 45^o Centigrade.

Vegetation is very sparse and is mostly confined to the wadis. The only extensive area of dense vegetation is Feiran Oasis; elsewhere, wells and springs may have clusters of palms around them. Uncultivated vegetation consists of occasional acacia trees, along with widely interspersed shrubby plants. Only a small fraction of a percent of the surface is covered by vegetation.

The southern part of the Sinai peninsula has very rugged topography. Areas of igneous and metamorphic rocks are hilly and mountainous. Wadis and the associated lacustrine beds are essentially the only flat areas. The ruggedness of the topography affects remote sensing studies, since western slopes would be in shadows in Landsat images. The relief

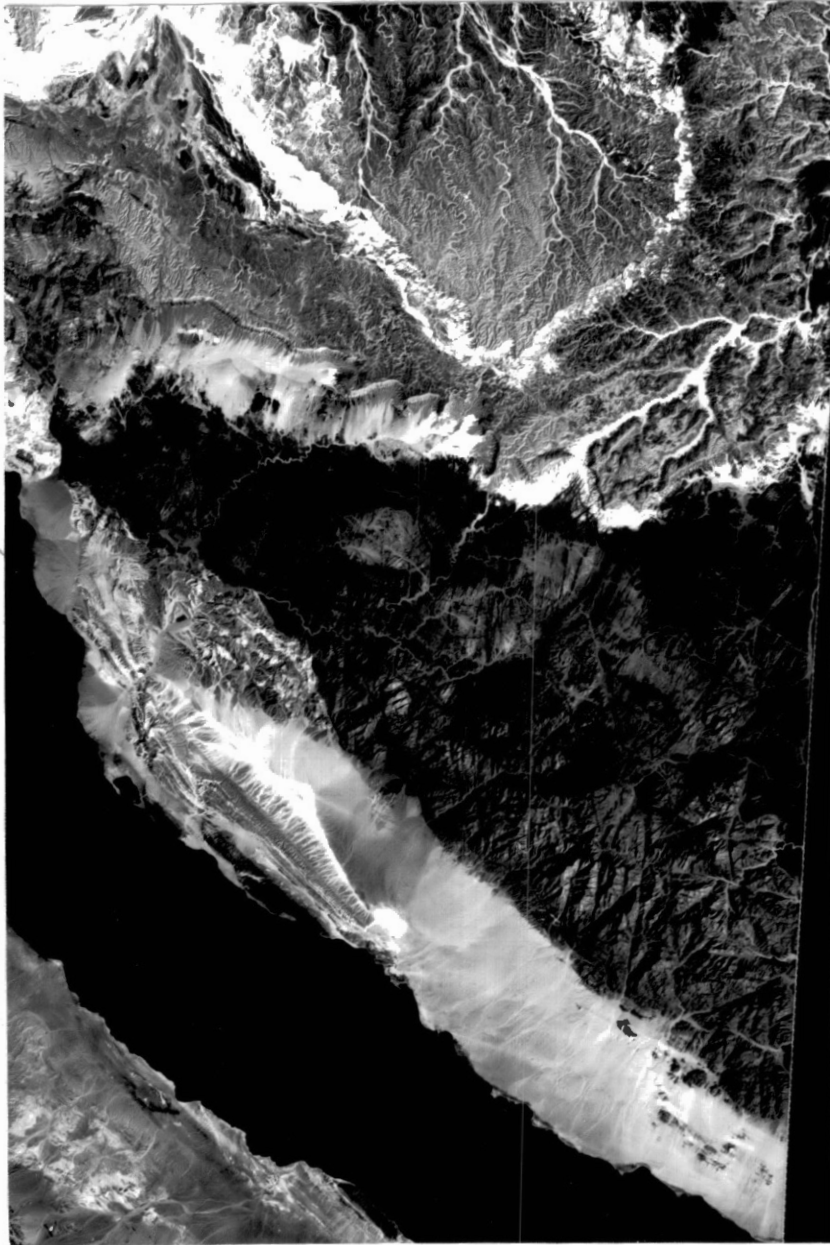
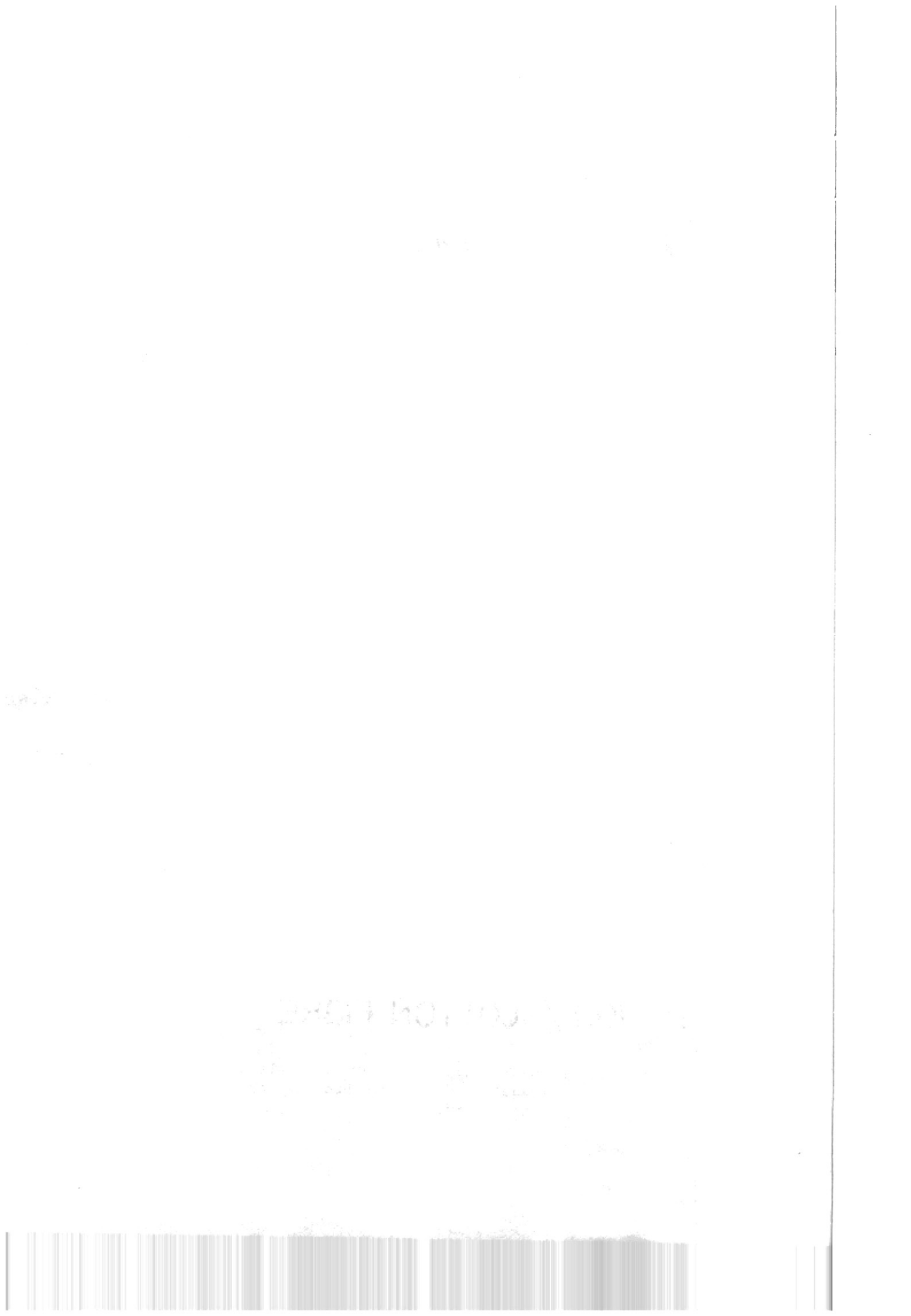


Figure 1. LANDSAT Image 1109-07493 (Not All of Image Shown). Image Provided by Cities Service Co.



also hampers travel, restricting it to the wadis and coastal plains or the air.

CHAPTER III

PREVIOUS INVESTIGATIONS

A. Geology of Sinai

The first comprehensive investigations of the geology of southern Sinai were done early in the 20th Century by Barron (1907), Hume (1909), and Ball (1916). These were studies of the topography and petrology of major segments of the area. In 1948, Davey published an account of mining activities, past and present, in Sinai. Several studies were published in the 1950s on the Sinai copper deposits; these included the study by Abdel Naser and Chukri (1954), which gave brief descriptions of the known occurrences of economic minerals in southern Sinai and included sketch maps of the Regeita deposits. El Shazly, Abdel Naser, and Shukri (1955) studied the mineralogy of the copper deposits of Sinai; they found hypogene malachite and a number of its oxidation products; especially azurite, chrysocolla, and chrysocolla. Hilmy and Mohsen (1965, 1966) listed the copper minerals found in the sandstones immediately north of the igneous and metamorphic rocks, and described the geology of the copper-bearing localities of that area. These sandstones were described in considerable detail by Soliman and El Fetouh (1969). Certain areas of igneous and metamorphic rocks in Sinai were described by Schurmann (1966) in his study of Precambrian rocks in the vicinity of the Red Sea.

The plate tectonics of the Red Sea area have been studied in some detail; the plate tectonics of Sinai were addressed in several of these studies. Robson (1971) gave a comprehensive summary of the plate tectonics in the Gulf of Suez area. Degens and Ross (1969) edited a volume on the hot brines and associated mineral deposits in the Red Sea, in which the plate tectonics of the area were also discussed. The studies mentioned above are concerned with Cenozoic activity. Shimron (1980) published a paper on the plate tectonics of Sinai in the Precambrian; his conclusions are discussed later in this thesis.

The Egyptian Remote Sensing Center published a study by E. M. El Shazly et al. (1974) which was a remote sensing study of Sinai and included maps of the geology, drainage, lineaments, and economic geology of the peninsula; the maps have been revised several times, the latest being in 1982.

A study was made in Israel and Sinai (Nathan, Bentor, and Wurtzburger, 1970) in which a vein of palygorskite was described 5 Km south of the mouth of Wadi Hebran. It was within a fault zone and accompanied by signs of hydrothermal activity such as quartz veins and epidotization.

Wachs, Arad, and Olshina (1979) made a study for locating ground water in the Santa Catherina area by geophysical methods. They found that water flow occurred mostly along joints in bedrock rather than in alluvial fill.

B. Landsat Methods

Exploration for minerals by using Landsat is something that started as soon as the ERTS-1 was launched in 1972. The efforts to detect hydrothermal deposits rely on two principles: 1) the mineralizing fluids

alter a fairly large area of rock and change its spectral reflectance properties; 2) there is often structural control of mineralization.

Two studies were very influential in determining methods used for my study. These were studies performed in areas known to be mineralized, and were thus evaluations of how mineralization can be detected by remote sensing. The primary emphasis in the study by Rowan et al. (1976) was spectral reflectance; in the study by Nicolais (1976), the emphasis was on structural control.

Rowan and his co-workers studied the Goldfield area of Nevada. This area consists of Paleozoic shales and chert and Mesozoic granitic rocks overlain by Miocene volcanic rocks. The Miocene volcanics have been extensively altered and mineralized. Alluvium of Quaternary age covers approximate half the area, with the Miocene volcanics forming 95% of the rest of the outcrop. Vegetation is sparse, covering 10-20% of the valleys.

In the Goldfield study, a number of manipulations of the Landsat image were tried in an effort to distinguish altered areas from the rest of the area. Both standard and stretched single-band images proved to be inadequate, since alluvial and tuffaceous sediments showed reflectance patterns similar to that of altered areas. False color composites, both stretched and unstretched, proved to be no better. Color band ratio images were then tried, and proved to be useful, especially when stretched. Blue was used for the ratio of band 4 to band 5 (4/5), yellow for 5/6, and magenta for 6/7. Diazo transparencies, clear when a pixel value is 0, were much more useful than merely using color filters and allowed discrimination between altered areas and alluvial areas. Mineralized areas were green or sometimes red to brown; this indicates

these areas have high values in the first two ratios and low to medium values in the third.

The Goldfield study is based on the fact that the minerals characteristic of hydrothermally altered rocks have reflectance spectra very different from those of unaltered rocks (see Figure 2). The methods used in that study should thus be applicable to other areas of unvegetated igneous rock, terrane irrespective of the variety of igneous rock.

Stephen Nicolais prepared a study to test the importance of lineaments and their intersections in discerning mineralized areas. The Landsat image used was of central Colorado; this area covers a number of mineralized areas, including Cripple Creek, Breckinridge, Climax, Leadville, Bonanza, and quite a few others. He developed a lineament map of the area, which was used to select target areas. Assumptions used to find the targets were: (1) metallic mineral deposits were being sought; and (2) faults and shear zones had affected ore deposition. He found 40 targets, and from this group selected 10 target areas that seemed best based on complexity, type, and strength of lineament intersections and the presence or absence of curvilinear or circular features (indicating stocks or other intrusives). Each of the 10 areas had a 14-kilometer diameter, and the presence of curvilinear or circular features was considered to be the most influential in selection of the targets. Five of the 10 areas coincided with known mining districts: Bonanza, Cripple Creek, Tomichi, Breckinridge, and the Leadville-Alma-Climax area.

Nicolais provided the lineament interpretation to 15 professors and graduate students at the Colorado School of Mines, and asked them each to select 10 circular, 14 kilometer-diameter target areas by using the same assumptions he had used. The results were that 8 areas were picked

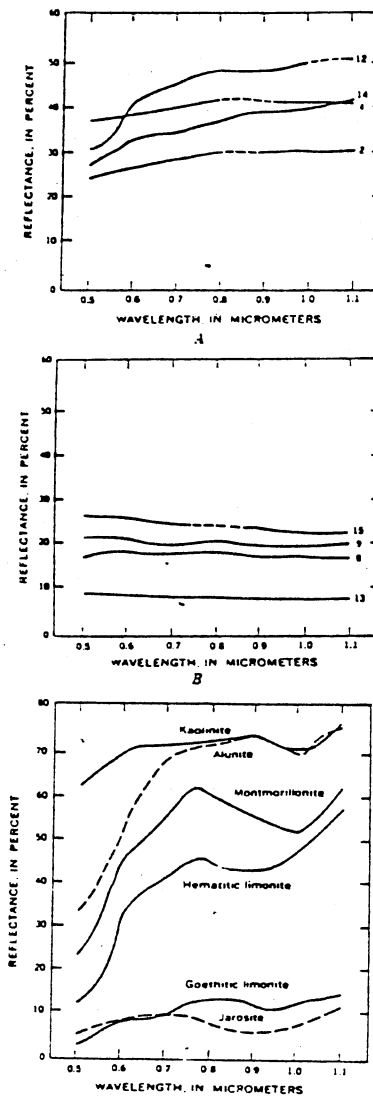


Figure 2. Reflectance Spectra of Various Igneous Rocks (Top and Middle) and of Alteration Minerals (Bottom) From Rowan et al., 1976

by most of the group and 5 of these coincided with known mineral districts. Four of the 5 had been picked by Nicolais in Phase I. The probability of 5 people selecting the same successful target area is 1 in 1.4×10^7 , indicating that chance played little role in selecting target areas.

Other studies have also linked lineaments to metallic ore deposits. Anderson and Smith (1975) observed that the area of greatest intersection of linear features with curvilinear features (on a Landsat image of north central Utah) coincided with the area of major metallic mining activity. Out of 45 mining districts or areas, 15 (5 of them major) were bisected by a lineament; 7 (one major) were at the intersection of 2 major lineaments; 2 were at the junction of a curvilinear feature and a lineament. Only 5 were not near an observed lineament when mapped at 1:1,000,000 and again at 1:250,000 scale. "Major" was not defined for any term indicating lineament and mining district.

Moore (1976) noted that a prominent lineament in the Arabian Shield was related to mineralization. The lineament coincided with the Al Amar Fault; this shear zone apparently had allowed large amounts of fluid to pass through, causing widespread hydrothermal alteration; however, there was no direct evidence of the fault acting as the direct access for metal-bearing fluids.

Offield et al. (1977) used a Landsat image to map lineaments in an area of southern Brazil. A lineament--a rather wide one--that had previously not been detected was found; the lineament zone has deposits of gold, tin, and copper.

Aarnisalo (1978) made a study of lineaments and mineral occurrences in Finland, to see if there was correlation. A total of 142 mineral

occurrences were plotted; 56 were in fracture zones, 52 were within 2 kilometers of fracture zones, and 34 had no recognizable association with fracture zones. The occurrences were listed as oxides (of iron, titanium, vanadium, and manganese), as sulphides (of copper, zinc, lead, iron, and molybdenum) and as nickel or chromium. All three classes had a tendency to be associated with fracture zones; nickel and chromium showed this trend to a strong degree.

O'Driscoll (1981) noted the presence of "structural corridors," which he defined as "relatively narrow belts or passages within which the density of lineament population is in marked contrast to that of surrounding areas." He saw these in gravimetric and magnetic plots as well as aerial photographs and Landsat images. He believed these corridors to be related to basement or bedrock disturbances. He also noted an association with mineral and energy resources; as examples, he discussed the goldfields of the Copper Basin in Australia, the mineral belt of western Colorado and eastern Utah, and the salt anticlines of the Paradox Basin.

Raines (1978) performed a study of northern Sonora, Mexico that used both lineament studies and the techniques used by Rowan (to locate hydrothermally altered areas in Nevada) to search for porphyry copper deposits. A lineament map was drawn from an image in band 5 and a statistical analysis was made using a 90 percent significance value. Three statistically significant trends were found: west-northwest, north-northwest, and northeast. Intersections of lineaments on these differing trends were contoured on a frequency basis. Then, areas of hydrothermal alteration were located by the process used by Rowan et al. (1974) at Goldfield, Nevada. There was a frequent association of altered

areas with the northeast flank of areas which had a high density of lineament intersections.

Garson and Krs (1976) noted several sets of lineaments in southeast Egypt. One set, trending $N 60^{\circ} E$, is perpendicular to the Red Sea rift; the other, parallel to the Red Sea, showed up on both Landsat images and aeromagnetic maps. They noted that intersections of these two sets were in several cases significantly mineralized.

CHAPTER IV

GEOLOGY

A. Geologic History of Southern Sinai

The geologic history of Sinai is known in only fairly general terms, owing to the lack of detailed regional studies. There have been two comprehensive summations of the area's geologic history; Shimron (1980) related events and lithologies to a plate tectonics model, whereas Schurmann (1966) mainly discussed lithologies. Schurmann's terminology is used in the present study but the narrative is based on Shimron's theories. A geologic column of Sinai's Precambrian rocks is shown as Figure 3; maps of the area's Precambrian geology are shown in Figures 4-12.

The oldest rocks of Sinai are those of the Mitiq series; these are mainly paragneisses and orthogneisses; Siedner et al. (1974) dated these rocks at 1100 my. The units included in the Mitiq Group include the Feiran-Solaf Belt, the Elat-Neviet Belt, and the Qenaia formation, according to Shimron. Gneisses, schists, and migmatites are the dominant lithologies; metamorphism is amphibolite to granulite facies. There is evidence of much deformation and even local melting during the Kibaran orogeny. Some lamprophyre dikes are in these rocks, and pre-date all other rocks; Shimron speculates that these may be related to the opening troughs in which geosynclinal sediments (Shadli Group) were deposited.

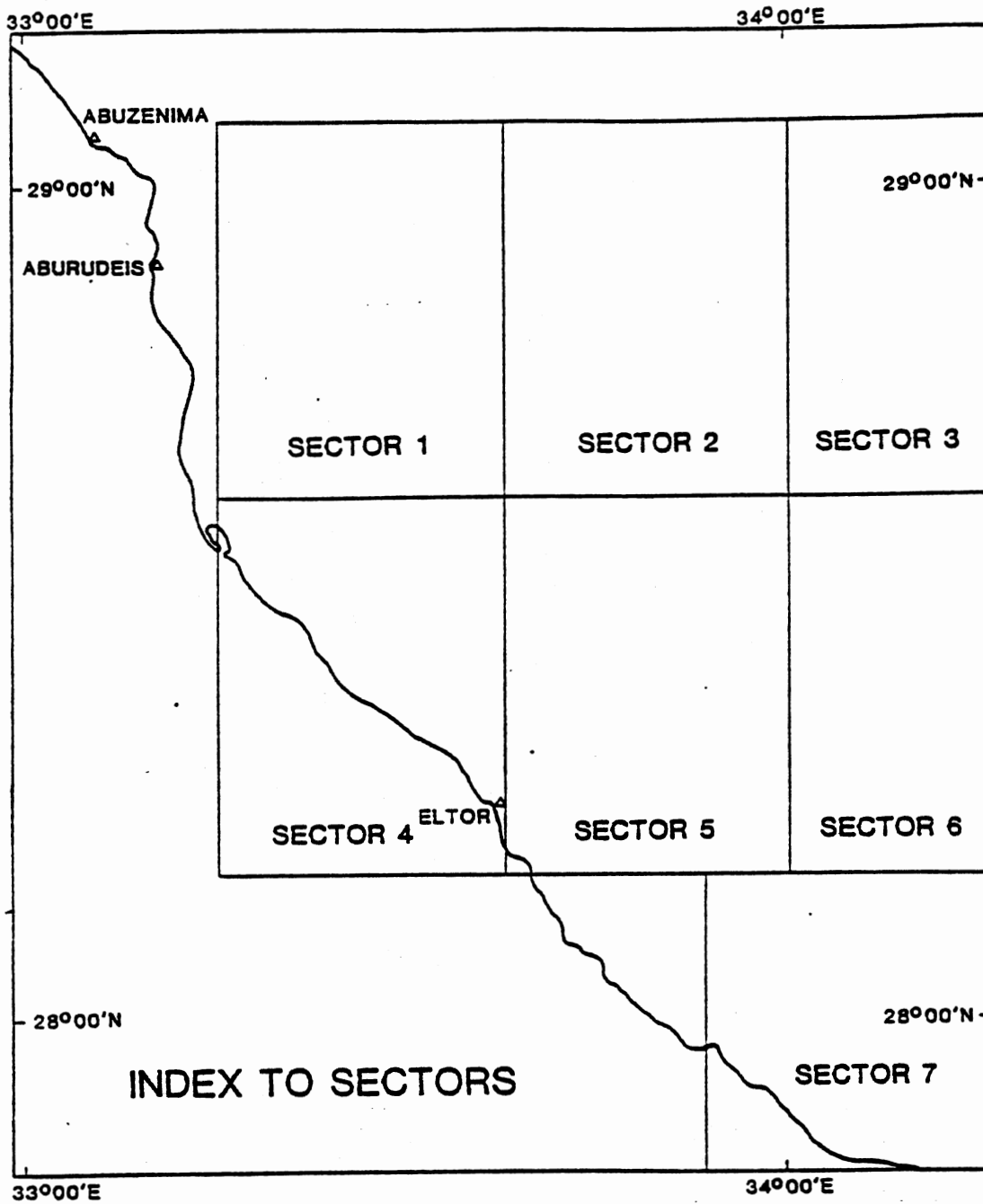


Figure 4. Index Map, Geological and Lineament Map Sectors

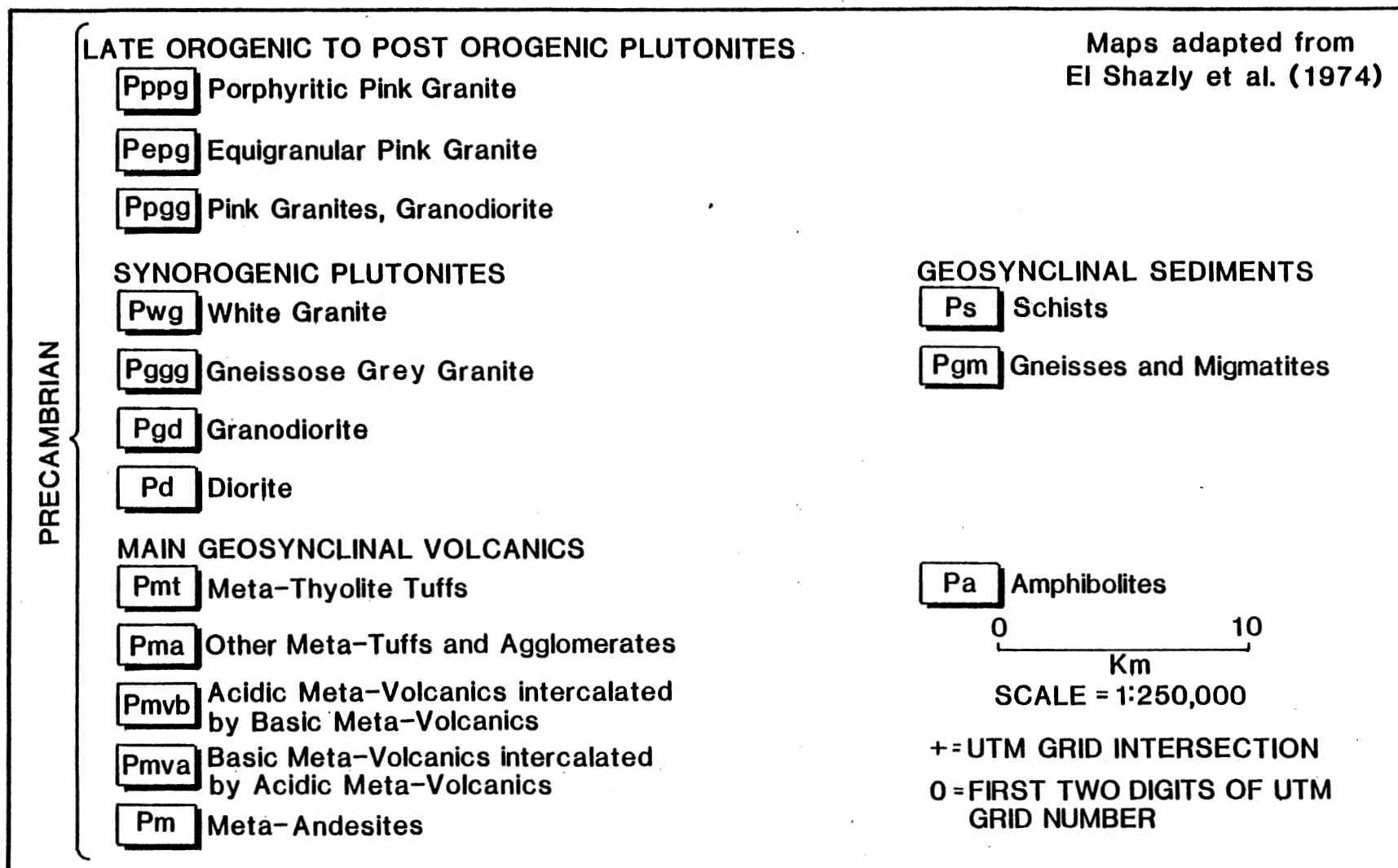


Figure 5. List of Symbols, Figures 6-12

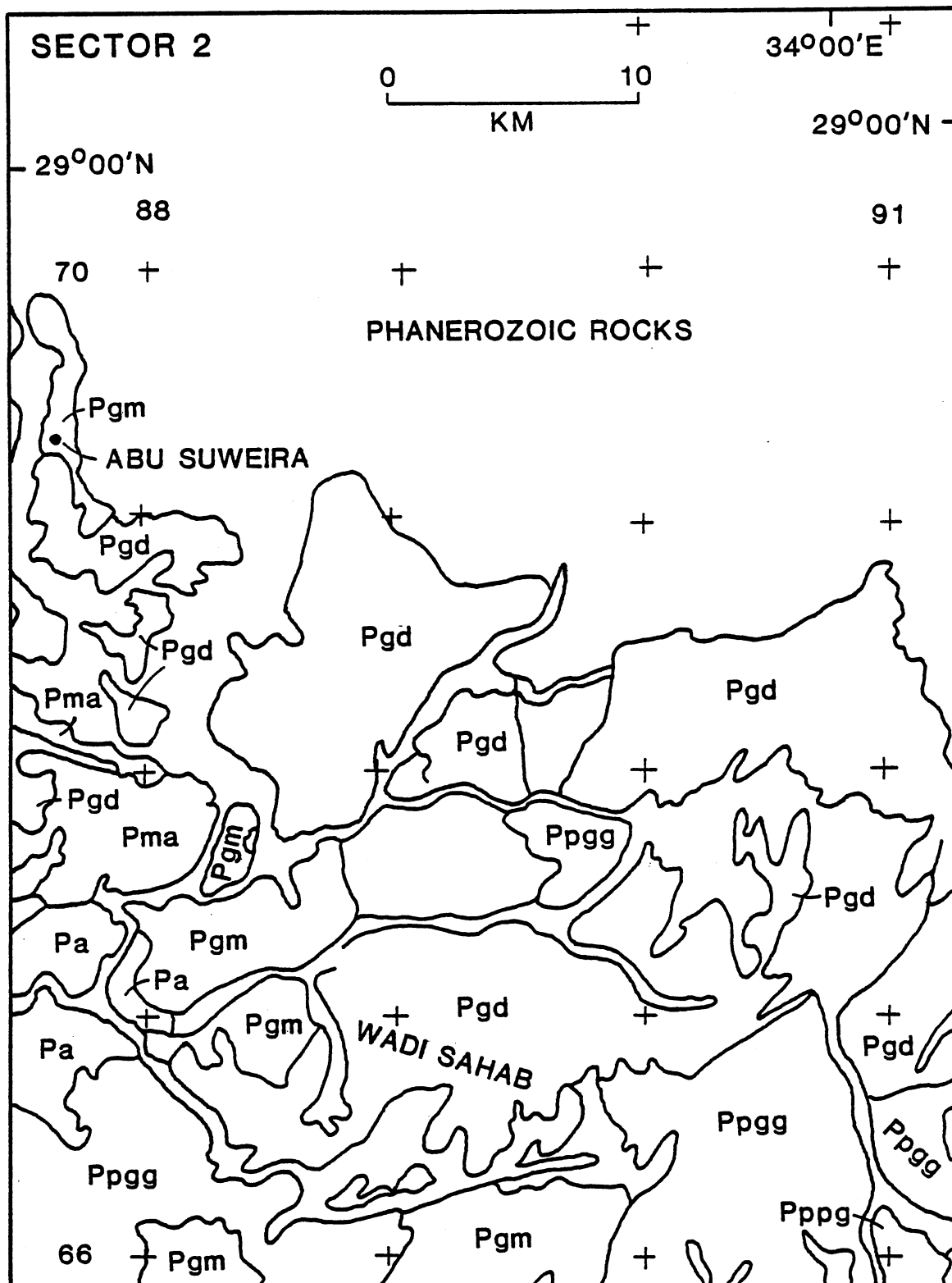


Figure 7. Geologic Map of Southern Sinai Precambrian, Sector 2 (See Figure 5 for Legend)

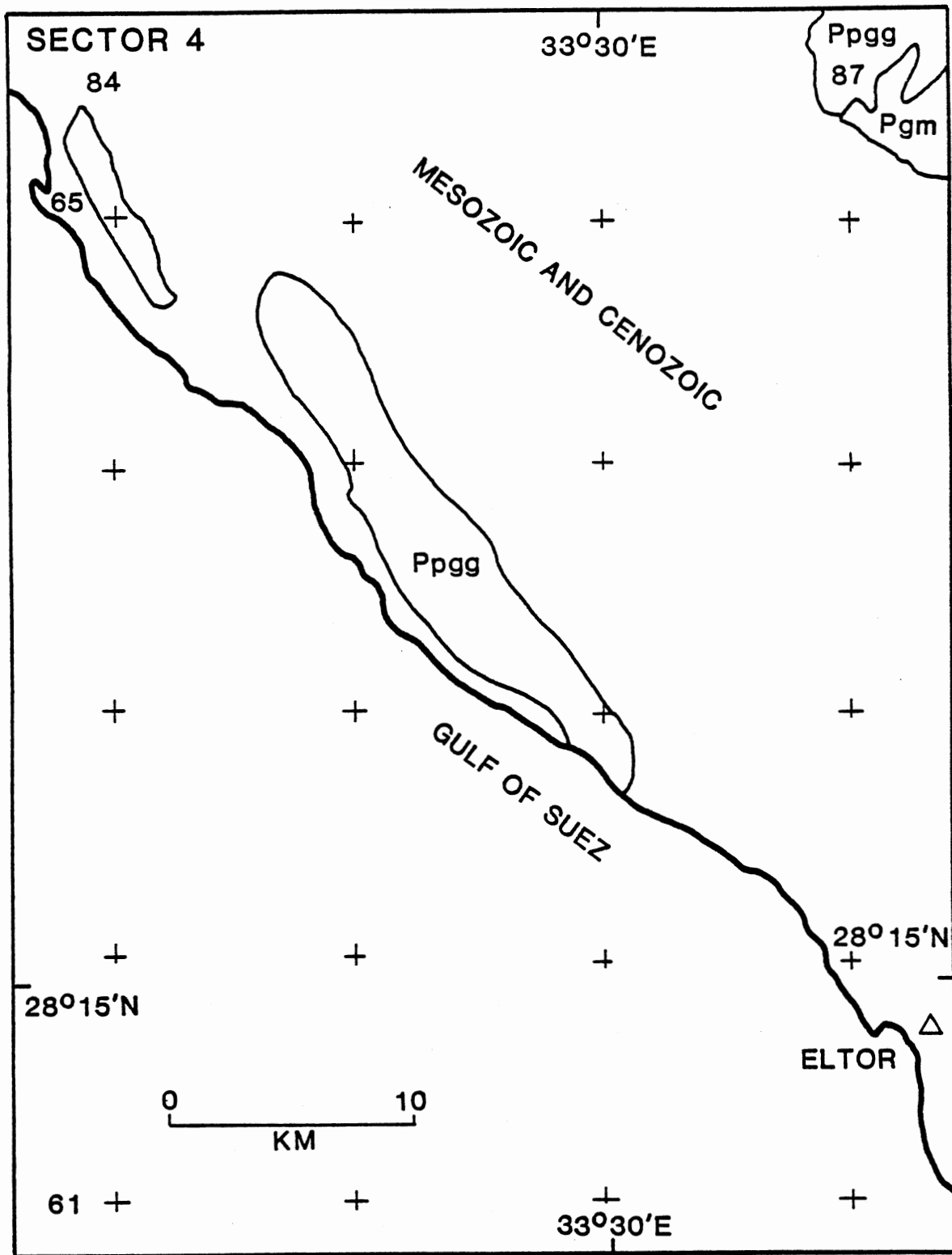


Figure 9. Geologic Map of Southern Sinai Precambrian, Sector 4
(See Figure 5 for Legend)

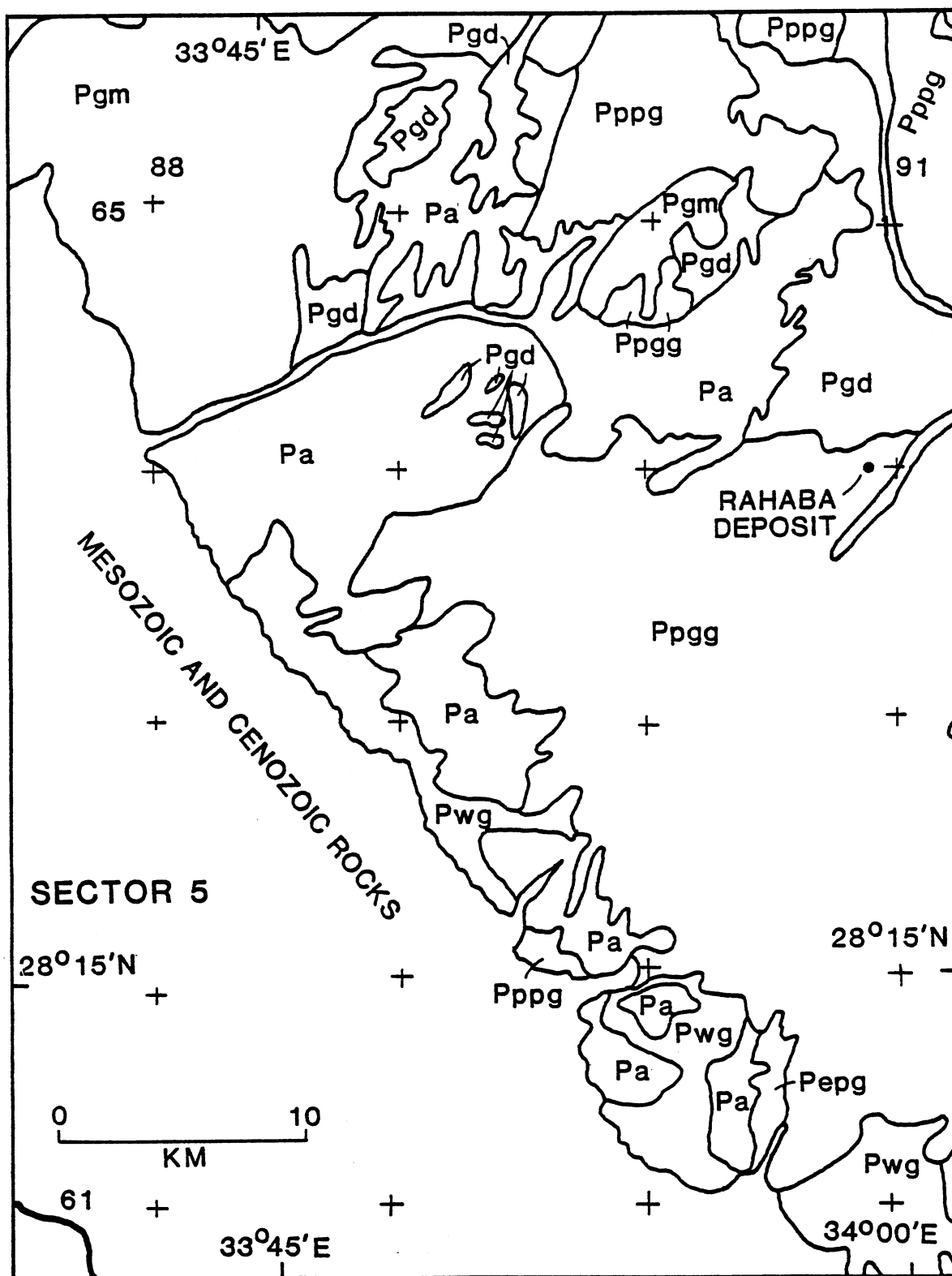


Figure 10. Geologic Map of Southern Sinai Precambrian, Sector 5
(See Figure 5 for Legend)

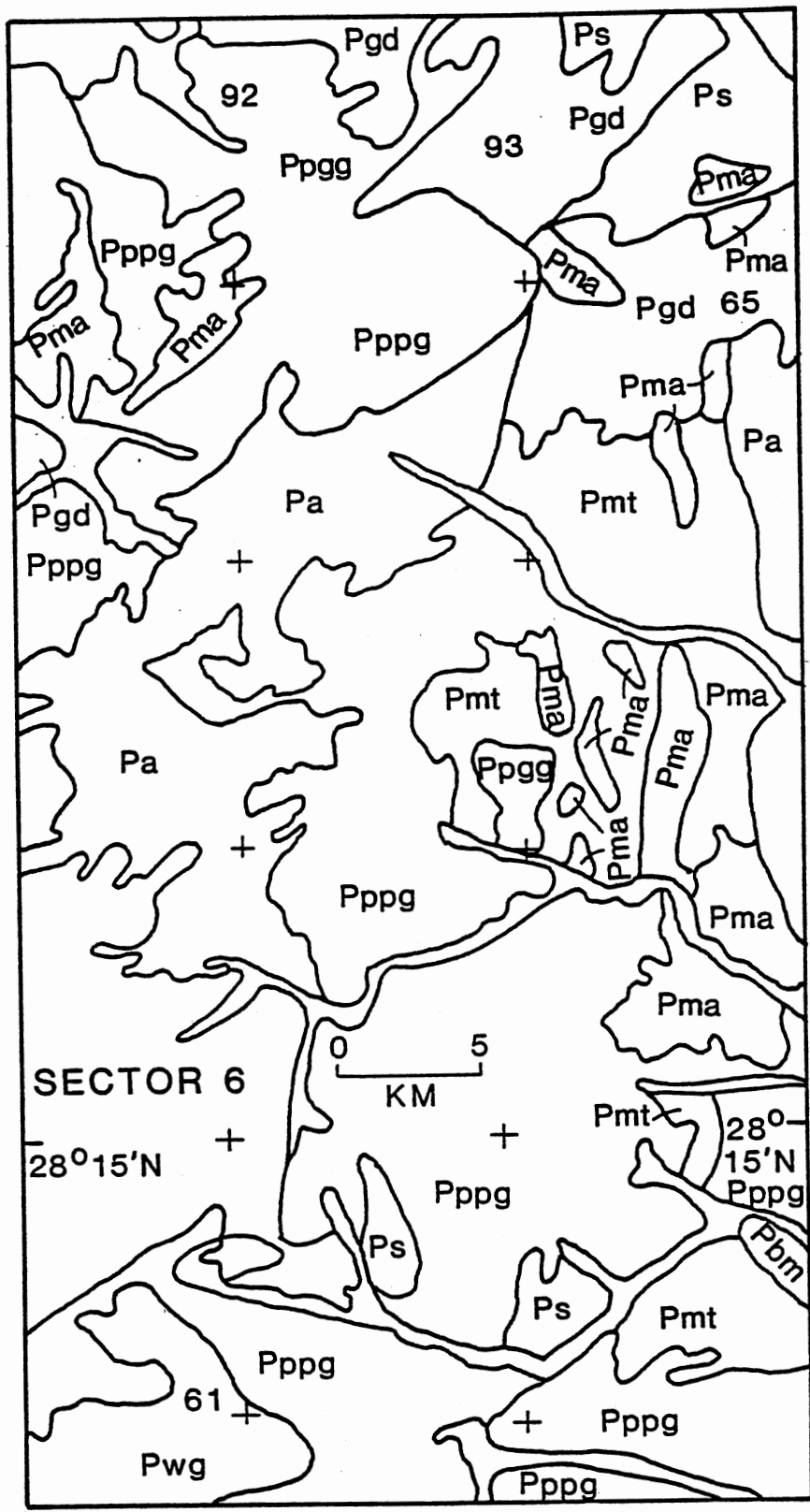


Figure 11. Geologic Map of Southern Sinai Precambrian, Sector 6 (See Figure 5 for Legend)

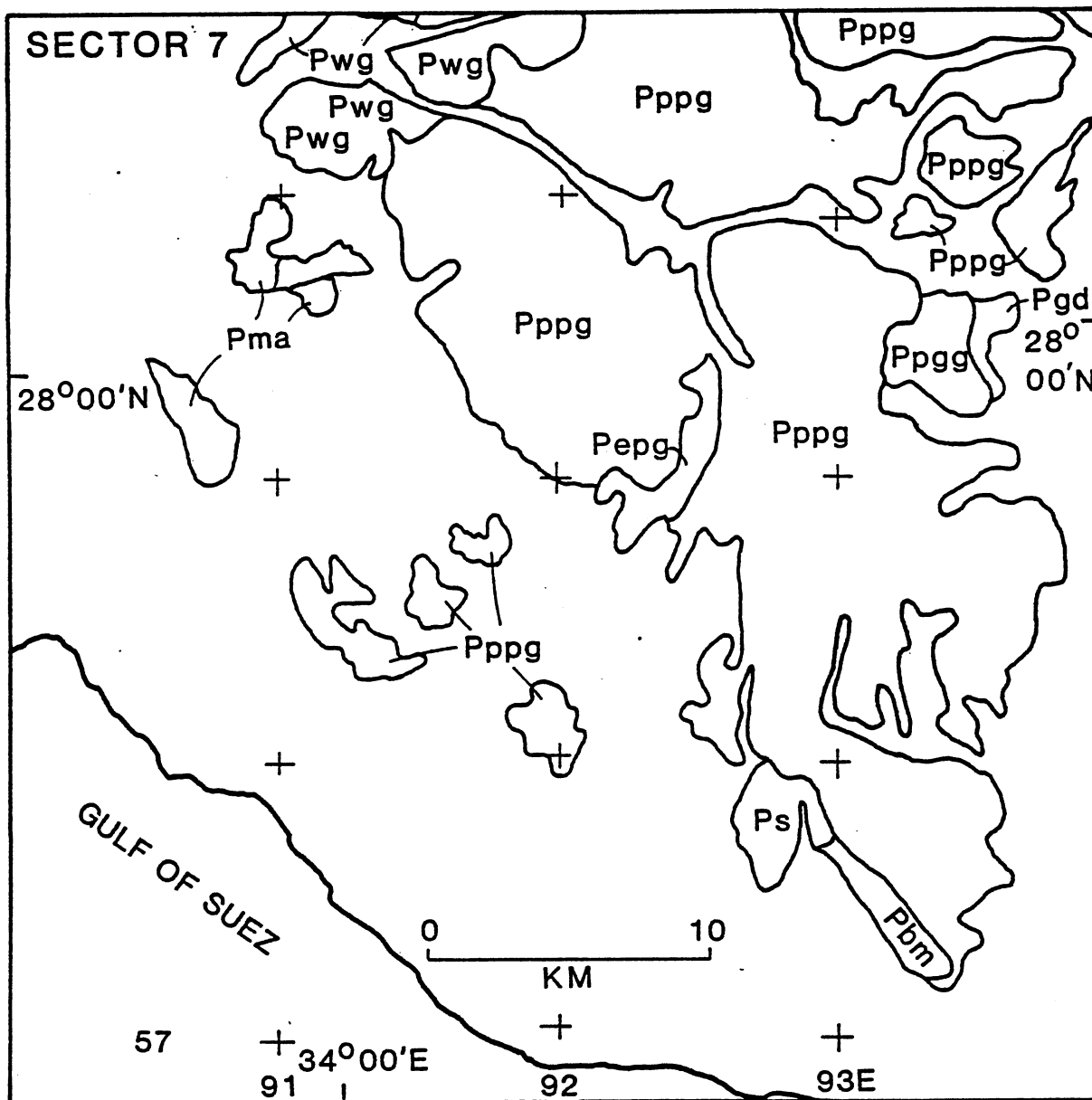


Figure 12. Geologic Map of Southern Sinai Precambrian, Sector 7 (See Figure 5 for Legend)

The Kibaran orogeny took place in north and central Africa about 1,000 million years ago, and may be responsible for the next oldest assemblage of sediments. These are called the Shadli Group by Schurmann; they have been much better described by Shimron who calls them the Sinai Supergroup, divided into the Sa'al and Kid Groups. Quoting Shimron, these sediments exceed 20,000 meters. The Sa'al Group consists of basalts, greenstones, and rhyolites (and the pyroclastic equivalents of those three) as well as marble, conglomerates, arkoses, quartzites, and porphyroblastic phyllonites. This geosynclinal sequence is also represented by some plutons of "granitic and granodioritic cataclastic augen gneisses and subsidiary quartz diorites" (Shimron, p. 443). The Kid Group has a very diverse lithology of geosynclinal affiliation; hornfels, marble, greywacke, chert, ignimbrite, conglomerate, pyroclastics, slates, and phyllites are present; andesite and rhyodacite are also present. Turbidite beds are present, as are graded beds.

The two groups have been divided by Shimron into several formations. The Sa'al Group consists of the Zrara Formation (slate, arkose, quartzite, and conglomerate) has been metamorphosed to a greenschist facies as has the Agramiya Formation (basalt, tuff, rhyolite, and ignimbrite). The Kid Group consists of: the Farr Formation (slate, greywacke, quartzite, marl); the Heib Formation (flows, volcanoclastics, conglomerate); the Umm Zariq Formation pelagic facies, schists, greenstones); and the Dakab ophiolite, which consists of metaperiodotite and layered gabbro. All the Kid Group has been metamorphosed to an amphibolite facies, although parts of the Zrara may be only greenschist. Shimron interprets the Farr Formation to be a shelf facies, with the slate being in part an algal slate; ash and other volcanic material in this formation indicate

the proximity of volcanic activity. The Umm Zaraf, on the other hand, with a pelitic-flyschoid sequence, is labeled as a deep-water sediment, probably deposited in an inter-arc or marginal basin.

During the Kibaran orogeny, plutons of dioritic or quartz dioritic composition were intruded, along with some gabbro, quartz monzonite, and granodiorite.

In summary, Shimron describes the Sinai Supergroup as the northernmost segment of an island arc sequence formed by the convergence of two plates, with the northern plate being subducted. The different formations represent different phases of the activity and are more a geographic sequence than a time sequence; in other words, they are approximately contemporaneous, but were formed at different areas of the converging plates.

After the Sinai Supergroup comes the Ferani Group, corresponding to the Dokhan of Egypt. In Sinai, these rocks are calc-alkaline flows, pyroclastics, ignimbrite, and conglomerate. Metamorphism has progressed to the greenschist facies. These sediments may have been deposited in intracratonic basins. An age of roughly 700 my is given to these rocks.

The Pan-African event gave rise to most of the granite that dominates southern Sinai. The sequence of events is: emplacement of calc-alkaline plutons; a volcanic episode (Catherina volcanics); and alkaline pluton emplacement.

The present phase of plate tectonic in the Sinai started about 26 million years ago (Girdler, in Degens and Ross, 1964, p. 42) when the Red Sea graben started to open. At the north end the graben branched; the eastern branch, the Gulf of Aden, displayed sinistral shift, while the western branch, the Gulf of Suez, displayed dextral shift.

Alternate names for these rift zones are Dead Sea Rift and Clysmic Rift, respectively. The African plate is, in relation to Sinai, rotating clockwise while the plate on which Arabia is located is rotating counter-clockwise. A map showing the plate tectonics of the Sinai area is shown as Figure 13.

The movements described above have had several effects upon Sinai. Fracture patterns in the Precambrian rocks are oriented (in large part) parallel to the two rift zones which are shown in Figure 14. There are fault--block mountains on the Gulf of Suez coast that are the result of rifting. Basaltic dikes of Miocene and Oligocene age are abundant in Sinai. Finally, transcurrent faults have been traced from the Gulf of Suez into Sinai (Abdel Gawad in Degens and Ross, 1969).

Several occurrences of metal-rich ocean-bottom sediments are associated with geothermal brines in the Red Sea south of Sinai. Metals which are present in significant amounts include lead, copper, and zinc among others. Lead isotope ratios indicate that the deposits are of extremely young age, in essence of zero age. Chalcopyrite and sphalerite have been identified in the sediments.

B. Lineaments and Their Relationship to Tectonics

The lineaments in Sinai (as seen on the Landsat images and shown in Figures 26-32) consist of fractures (including faults), lithology changes, dikes, and straight sections of wadis. The last two are often themselves manifestations of faults or fractures. Dr. Raafat Misak stated that wadis in the area under investigation were usually along faults; our own observations agreed with this statement, since lithology was often different on opposite sides of a wadi. Remnants of basalt

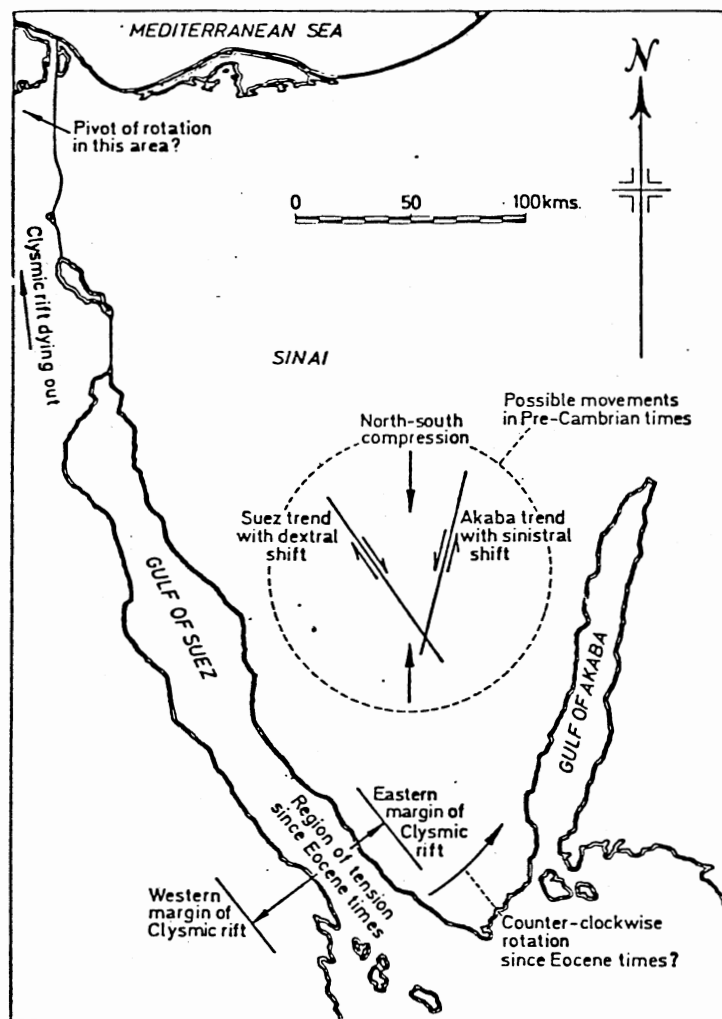
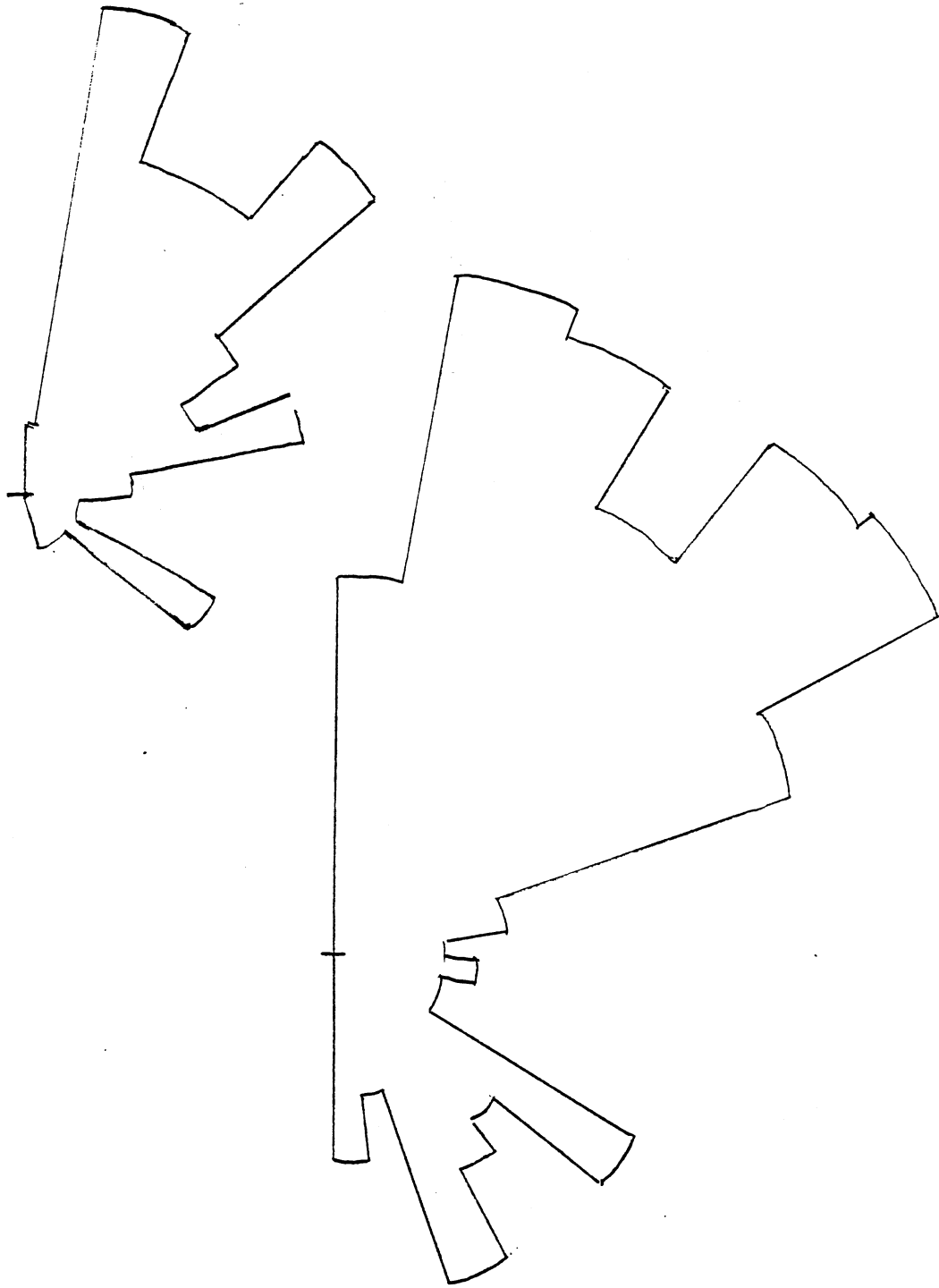


Figure 13. Plate Tectonics in the Sinai Region (From Robson 1971)



A. Salman, 1982



B. This study

Figure 14. Lineament Directions in Study Area

along the walls of wadis indicate that basaltic dikes may also be related to the faults. Lithology changes are also often indicators of faults, thus making it likely that practically all lineaments in the area are related to faulting.

The origin and date of the fracturing can be derived to some extent from the fracture density and the extent of particular fractures. An examination of the satellite imagery shows that most fractures do not cross the contact between the Precambrian outcrop and the younger rocks. This would indicate that most of the fractures are probably Precambrian and definitely Pre-carboniferous. It should be kept in mind, however, that some dikes of Miocene age traverse the area; two examples are referred to in the literature as the Ras Wata Dike and the Abyad Dike. This late episode of fracturing may be related to the opening of the Gulf of Suez and the Gulf of Akaba. Robson (1971) states that this faulting was initiated in the Oligocene and continued until after the Miocene, but that igneous activity associated with the Cenozoic faulting was confined to the Oligocene. Robson also states that the Cenozoic faults affecting the Precambrian in Sinai had mostly vertical movement. His rose diagram of the fault trends in the Sinai Precambrian shows a very definite tendency for faults to parallel the Gulf of Akaba, and a weaker but still prominent tendency to parallel to the Gulf of Suez. Rose diagrams of lineaments seen on Landsat imagery and compiled by Salman (1981) and by myself agree with that of Robson (see Figure 2).

The fact that many fractures parallel the Gulf of Akaba and the Gulf of Suez should not be taken as evidence that these are associated with the rifting that has occurred in Cenozoic times, unless they are occupied by dikes that have been dated as Cenozoic. In Precambrian

times the Sinai land mass underwent north-south compression; Shimron (1980) offers evidence of collision with and partial subduction under another land mass. The result was a set of fractures at 60° angles to the direction of compression.

C. Hydrogeology

There are no permanent streams in the study area; ground water is the only source of water. Recharge occurs as rain is quickly absorbed into the alluvial material in the wadis and into joints and fractures.

Fracture patterns are being used by Dr. Raafat Misak in the area under study to locate ground water. The intersection of a fracture by a basaltic dike (forming a barrier to ground water movement) can be used to locate areas of high yield; likewise, a dike crossing a wadi can create a subsurface dam that impounds water beneath the surface of the alluvium. The depth to water in the wadis and fractures ranges between 3 and 40 meters. Yield of the wells is up to 30 cubic meters (Misak, written and oral communications).

Misak characterizes the water as being of very good quality, low in mineral content. The ground water in the area of St. Katherine is very potable, with no undesirable taste. The water is susceptible to pollution by animal and human waste products; the extent of actual contamination, if any, is unknown. The writer does not know of any analyses of metal content in the ground water of the area.

The application of remote sensing to water location, by detecting fracture patterns, is obvious. The extent of such use is unknown.

D. Known Copper Deposits and Mines in Sinai

Copper deposits are known from a number of areas in Sinai; however, exact locations (such as latitude and longitude) are essentially non-existent in the literature. At Sarabit, the deposits are in sedimentary rocks--sandstones previously thought to be Carboniferous in age but now identified as Cambrian and designated to be the Sarabit El Khadem formation. An effort to examine this locality in January, 1982, was thwarted by impassable buildups of sand dunes in the wadi leading to the deposit. El Shazly, Naser, and Shukri (1955) state that the copper minerals are carbonates and silicates occurring as thin beds in shale and in small scale faults. In an oral communication, El Shazly stated that notable alteration of the host rock was present; this was confirmed orally by Misak. The other localities in the 1955 report are in igneous and metamorphic rocks in fracture systems cutting the rocks themselves or the associated quartz veins. The localities listed were Samra, Regeita, Rahaba, Bathat Um Rebei, Suweira, Abu El Nimran, and Feiran. At Samra, silicates and carbonates are present; Abu El Nimran has carbonates predominant, but also has appreciable amounts of oxides and sulfides. The others have carbonates predominant with minor amounts of sulfides and oxides present. Minerals reported present were covellite, chalcocite, malachite, chrysocolla, azurite, and cuprite.

In the same report, the authors considered chloritization and kaolinization of the wall rock near the deposits to be due to the hydrothermal fluids responsible for ore deposition; otherwise, alteration of wall rocks was not addressed. At Abu El Nimran, the occurrence of tin and bismuth in the chalcocite led them to conclude that the deposit was hypogene.

Abdel Naser and Chukri (1954) listed several copper localities. These are summarized below: the report gave only extremely brief descriptions.

1. Abu Suweira (Wadi Seih). Malachite fills fractures in granite over a two meter length; the vein, in grey granite, is up to 20 centimeters wide.

2. Abu Zagatan. Very similar to Abu Suweira.

3. Wadi El Reshidia (Seih). A malachite--impregnated quartz vein two meters long and ten centimeters wide.

4. Khor Abu Rudeib. A malachite--stained quartz vein.

5. W. Tuwillieh. A malachite--stained quartz vein.

6. Wadi Nisryn:

-at Wadi Ezamia, several malachite--impregnated quartz veins.

-at Wadi Um Kobitat, malachite in quartz veins and in granite fractures.

-at Wadi Um Silli, a "basic vein" stained with malachite.

-at Wadi Maghar--like Wadi Um Silli.

7. Gebel Abu El Nimran area. Three quartz veins with malachite, covellite, and chalcocite. The area of mineralization is extensive.

8. Wadi Tarfa. A malachite--impregnated quartz vein one meter long and 10 centimeters wide, with several similar exposures nearby.

9. Bathat Um Rebei. Similar to Wadi Tarfa.

Hume (1906) mentioned copper occurrences in the southeast part of Sinai. At Wadi Nasb, at $29^{\circ} 08' N$, $50^{\circ} 55' W$ (probably a typographic error - $30^{\circ} 55'$ would be in Sinai, but not 50°) he mentions a report by Ruppell in 1822 ("Reise in Nubien, etc.") of workings in sandstone and a sample that when smelted yielded 18% copper and an odor suggestive of arsenic compounds.

Barron (1905) states that the Wadi Nasb veins, which were of "blue and green carbonate" have been completely worked out. He states that turquoise has been mined at Serabit el Khadim and Gebel Maghara; at the latter place the mines extended over an area of 1.6 by 0.9 kilometers. He also states that at Meghara the turquoise is in a purplish-grey bed of sandstone of Carboniferous age. He states that the best turquoise was in sand streaks, inferior turquoise being found along joints. The wadis in which the mines occurred are Wadi Qena and Wadi Sidri. Apparently the only igneous rock exposed is a basalt layer capping the hill, and Barron found no evidence of the turquoise being associated with it.

In a discussion of the Sherm El-Sheikh area, Sheta described the copper deposits at Samra. Malachite, azurite, and chrysocolla occur in fractures; the host rock is not specified. Gangue minerals are hematite, pyrite, quartz, and a pale green, fibrous amphibole. The mineralized zones and veins trend NW - SE and WNW - ESE, with some trending NNE - SSW; they dip at 75 - 80°. Sheta classifies the deposit as hypogene. He describes alteration of the wall rock as consisting of formation of chlorite, epidote, zoesite (sic), saussurite, and kaolinite.

Some copper mineralization is associated with the manganese deposits at Um Bogma. Malachite encrustations occurred on specimens of manganese ore collected by the writer at this locality.

The known deposits of copper in the igneous and metamorphic complex of Sinai display the same main characteristics. They consist of deposits in fractures and quartz veins and have as the main copper minerals malachite, azurite, and chrysocolla; sulfides are often present, but in minor amounts. Alteration of wall rock is minor, epidote, kaolinite sericite, and chlorite being the common indicators of altera-

tion. The evidence points to deposition of sulfides--chalcocite and covellite--by ascending hydrothermal solutions which also altered the rock adjacent to the fractures in which ore deposition occurred. Malachite, azurite, chrysocolla and other secondary copper minerals resulted from weathering of the deposits.

E. Description of Copper Deposits

Examined in the Field

El Tarr

The El Tarr locality consists of a biotite mica schist intruded by a white granite. An aphanitic dike with a strike of $N44^{\circ}E$ occurs approximately 50 meters east of the area of mineralization; the rock in this dike has been altered to such an extent that the original composition can no longer be discerned, but an intermediate (rhyodacitic or dacitic) composition is hypothesized (see Figure 15). Immediately around the granite intrusion, the rock is broken up to such an extent that a fault if it exists, can not be discerned (see Figure 16). However, two faults can be seen across the road; one is in the rock exposed in the hill that occurs at that point, while the other is expressed as a wadi (see Figures 17 and 18). If the traces of these two faults were extended, they would intersect at or very near the mineralized area. It must be kept in mind that the road is itself in a wadi which is mostly controlled by faults, so the locality is an intersection of three faults. The fault in the wadi would strike $N3^{\circ}W$, while the one in the hill parallels the dike; the road is approximately $N80^{\circ}W$ at the locality.

The copper mineralization was seen in both the granite and the



Figure 15. Aphanitic Dike at El Tarr



Figure 16. Granite Intrusion at El Tarr. Gr =
Granite, S = Schist



Figure 17. Wadi at El Tarr



Figure 18. Hill Opposite El Tarr Deposit. F =
Fault, D = Aphanitic Dike

schist, the entire area of mineralization extending perhaps 5 meters. The outcrop had obviously been to a minor extent; together with the shattering of the rock (perhaps by faulting, perhaps by the intrusion of the granite) the appearance of the rock is chaotic and conclusions about the structural relationships of the lithologic components are difficult to discern.

Section T-3 shows the contact between the biotite schist and the granite intrusion at El Tarr. The biotite schist has been extensively altered; most of the biotite has been altered to chlorite while most of the feldspar has been sericitized. Epidote is abundant. Quartz, comprising about 5% of the schist, occurs mostly as small grains which under crossed nicols have a mottled appearance. The granite consists of large grains of orthoclase (20%), quartz (40%), plagioclase (35%), and biotite (5%). The biotite has to a large extent been chloritized and the feldspars have somewhat sericitized. Alteration is more pronounced in the schist than in the granite. A chilled contact is apparent in the thin section; the grains go from one or two centimeters in the main part of the granite to a much smaller size--around three or four millimeters--at the actual contact. At the contact area the granite becomes somewhat enriched in chloritized biotite. It is in this area of increased biotite that a band of copper mineralization has developed; the minerals that have been deposited include covellite surrounded by malachite. Copper minerals also exist in the main part of the granite; in a thin section of this rock, large opaque grains consist of a brown anisotropic grain surrounded by chalcocite, which in turn is surrounded by malachite. In both cases, replacement of biotite and perhaps quartz has taken place (see Figure 19). The hand specimen of this rock is a black,

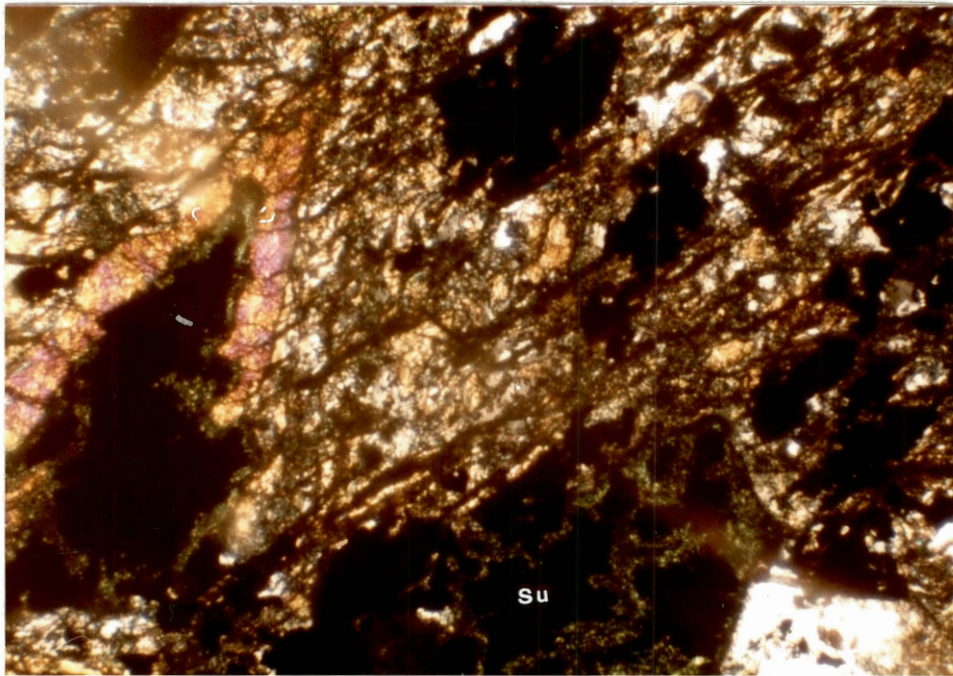


Figure 19. Photomicrograph of Thin Section T-3
Under Cross Nicols. Su = Sulfide

nonfriable mica schist grading into a white biotite granite; the chilled contact is visible but not especially prominent and alteration is not visible although the zone of copper mineral is very apparent.

Section T-7 is of the granite intrusion at a spot away from the contact zone. All grains are quite large, averaging around one centimeter along the longest axis. The hand specimen is a white biotite granite with gray quartz (40% of the rock), white plagioclase (25%), while orthoclase (30%), and black biotite (5%). A thin section of the rock showed sericite replacing feldspars (which were often zoned) and also showed chlorite replacing biotite. As described in the preceding paragraph, sulfides and malachite have replaced some of the quartz and biotite and the malachite stains the feldspar crystals.

The aphanitic dike at El Tarr is brick red and otherwise featureless in the hand specimen, except for faint suggestions of phenocrysts. The thin section shows a rock so severely altered that the original nature and constituents are not discernable. Although quartz is present, it is difficult to tell if the quartz is primary or secondary. Calcite occurs as veins perhaps a tenth of a millimeter thick and is obviously secondary. Hematite is extremely abundant. Assuming that the quartz is primary and that the calcite is the result of plagioclase alteration, a rhyolitic to dacitic composition is proposed for the rock.

Regeita Locality

The Regeita Mine, located approximately 5 kilometers southeast of the Saint Katherine Airport, consists of excavations along a fault in granite (see Figure 20). The granite, exemplified by sample SK-11, is a dark-red, hypidiomorphic-granular biotite granite. The rock contains

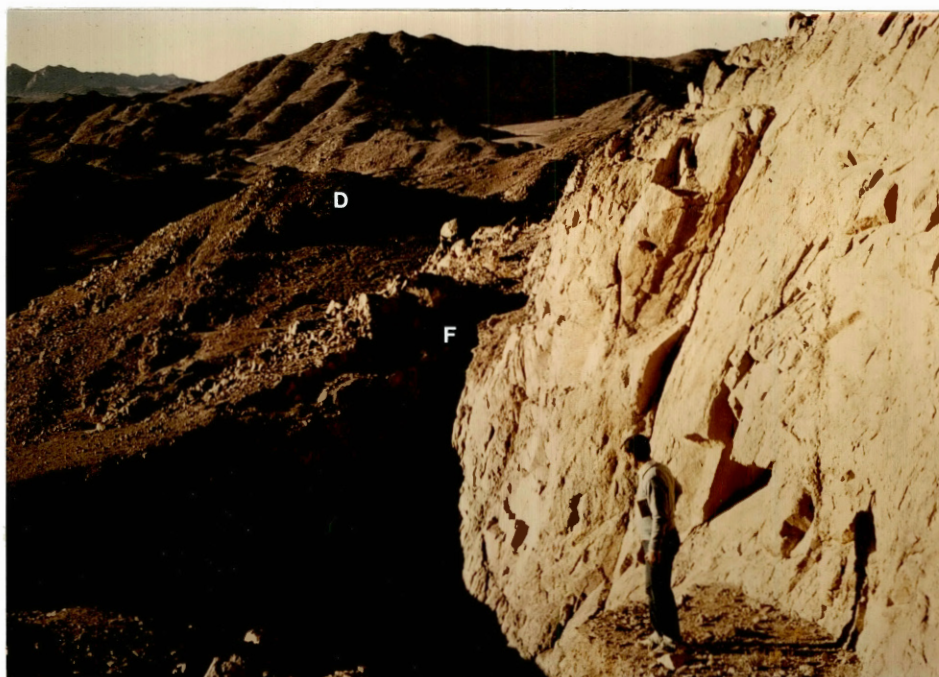


Figure 20. Regeita Mine, Looking North. F = Fault,
D = Dike

35% plagioclase and 35% orthoclase; the feldspars occur as subhedral grains, the plagioclase being white and the orthoclase red. Anhedral grains of clear, gray quartz make up about 20% of the rock, with biotite in the form of black laths being another 10%. A thin section of the rock reveals sericitization of the feldspars and chloritization of the biotite (see Figure 21). Apatite and zircon are visible in the thin section. Although the sample was collected only 3 meters from the fault, no sign of ore minerals can be seen and the rock is not visibly altered to the naked eye. SK-5, collected 20 meters from the fault, is very similar in both hand specimen and thin section.

The fault itself strikes N53°W and dips southwest at 78°; the direction of movement could not be discerned. The fault trace is on the average 1.5 meters wide and filled with a breccia in a clayey matrix. The clasts in the breccia are angular and average 3-5 centimeters; many are coated with blue minerals. The walls of the fault also are mostly covered with blue minerals. Analysis of the blue mineralization by the x-ray powder diffraction method indicated that chrysocolla is the main mineral present. Several clasts (R-2, R-3, R-4) were collected and later made into thin sections (see Figure 22). The specimen designated R-3 is a red granite with a blue amorphous coating on one side; vugs lined with blue or blue-green botryoidal mineralization can be seen on freshly broken surfaces. The plagioclase in the granite can be easily detected and is red; in the granites near the fault; the plagioclase is difficult to distinguish and is white. Other differences between this clast and the surrounding granite include sheared plagioclase crystals in the clast and a grain size averaging half that of the two SK samples. The evidence is that the clast has been transported, but the question

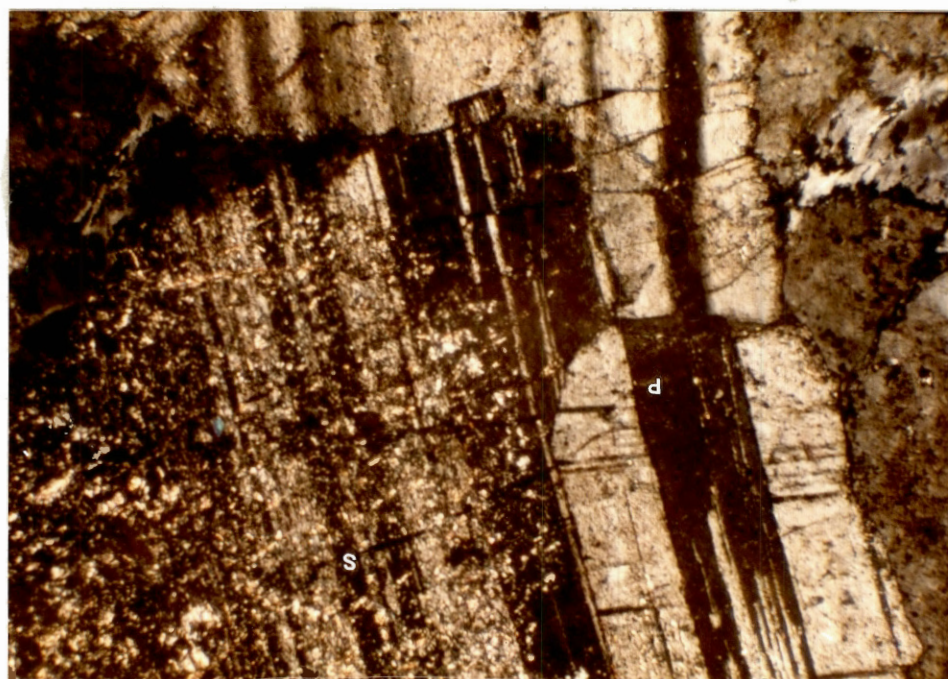


Figure 21. Photomicrograph of Thin Section of SK-11,
Showing Sericitization of Plagioclase.
Cross Nicols. P = Plagioclase,
S = Sericite

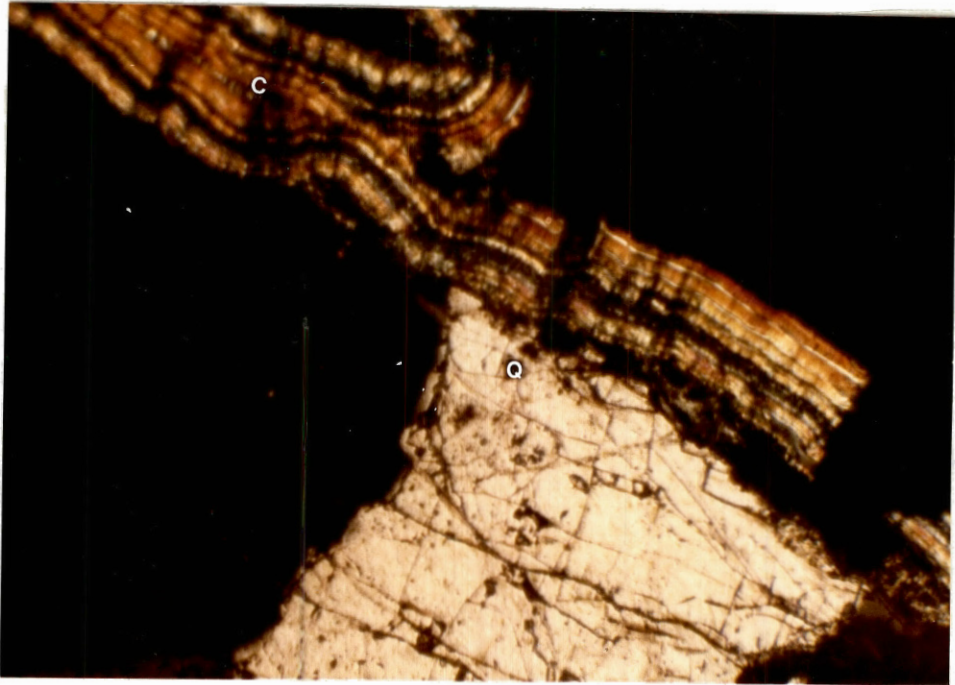


Figure 22. Photomicrograph of Thin Section of R-3, Under Cross Nicols, Showing Chrysocolla (?) Lining a Vug. Q = Quartz, C = Chrysocolla

remains as to how far. Other clasts from the fault breccia often resemble basalt, but in thin sections are too altered to identify. Assuming that all the clasts are altered by hydrothermal fluids, the question remains as to why R-3 shows only slightly altered feldspars while other clasts have been much more profoundly altered. Finally, some clasts are quartz. No quartz veins are to be seen in the vicinity of the fault, and the quartz clasts show signs of abrasion, thereby implying transportation. The conclusion that we reached is that the fault movement must have been mostly vertical.

A dike of dark reddish-brown aphanitic rock intersects the fault and forms the northern (and downslope) perimeter of the mineralization. The dike strikes $N38^{\circ}E$ and is essentially vertical. A thin section of the dike rock showed a profoundly altered rock in which the feldspars had been altered to the point of being unrecognizable, sericite having replaced them. Euhedral quartz crystal lined vugs; whether the vugs were a feature of the original rock or a product of alteration could not be determined. Vugs and fractures often were lined by a mineral having colloform texture and possessing a light green color in polarized light with high birefringence under cross nicols; some pleochroism was present. This mineral is tentatively identified as chrysocolla. The actual contact of the dike with the fault was obscured by rubble. The dike itself was unmineralized even a few meters away from the fault, as was the fault trace itself to the north of the dike. Misak, in an oral communication, stated that the dike was Jurassic in age.

Neither the dike nor the granite near the mineralized zone showed alteration to the naked eye, although epidote was visible along fractures in the granite. No hydrothermal veins were seen outside the fault

trace, not even quartz veinlets. This lack of quartz veins is characteristic of granitic areas in the Sinai. The presence of quartz in the fault trace, therefore, is made more notable.

In summary, the Regeita deposit consists of non-sulfide minerals deposited along a fault trace; within the fault trace, hydrothermal alteration has been extensive, but the surrounding granite shows little alteration even when adjacent to the fault. A dike of unknown but perhaps intermediate to basic composition forms the northern perimeter of the deposit, the southern perimeter not being seen by the investigators.

The presence of sulfides at Regeita was not seen in samples collected by the writer; however, they have been described from the locality. El Shazly, Naser, and Shukri (1955) stated that polished sections from the locality showed chalcocite to be the main and original copper mineral present.

F. Ore Deposition

In order to devise conceptual models of ore deposition, it was necessary to make several assumptions. The validity of the assumptions was based on published reports and on observations made in the field. These assumptions were as follows:

1. The copper minerals consisted of hypogene chalcocite and its alteration products (El Shazly, 1955).
2. The intersection of a fault or fracture with an aphanitic dike was conducive to ore deposition.
3. The aphanitic dike was a localizing factor.

At Regeita, the dike is later than the fault (see Figure 20), since it was not displaced where it cut across the fault. Since copper

mineralization was seen on only one side of the dike, deposition of copper was after emplacement of the dike. It is unlikely that the dike was the source of copper, since copper is seen on only one side of the dike and only in the fault. The dike itself shows extensive alteration and has euhedral quartz crystals lining vugs, but only at the fault intersection. X-ray powder diffraction analysis of the dike shows it to have calcic plagioclase; it is hypothesized that the reaction of the hydrothermal fluid with the plagioclase in the dike was the mechanism responsible for ore deposition.

El-Shazly, Abdel Naser, and Shukri (1955) state that the chalcocite at Regeita is hypogene. This writer sees two ways the chalcocite could have been deposited. A conceptual model of ore deposition is shown in Figure 23. Two alternative sources could have provided the copper served as a source for the copper in the hydrothermal fluid. First, descending meteoric water may have leached copper from the granite that the fault and dike transect; at depth, this water was heated and returned along the fault. Second, an intrusive body, not exposed in the area, may have provided copper and juvenile water which traveled along the fault. In both cases the dike would have served as geochemical stimulus to ore deposition. There is no direct evidence for the existence of an unexposed intrusive body.

No other locality provided enough information to determine the relation of the copper mineralization to the surrounding rocks. The writer is unaware of any published hypotheses on the nature of ore deposition in the area.

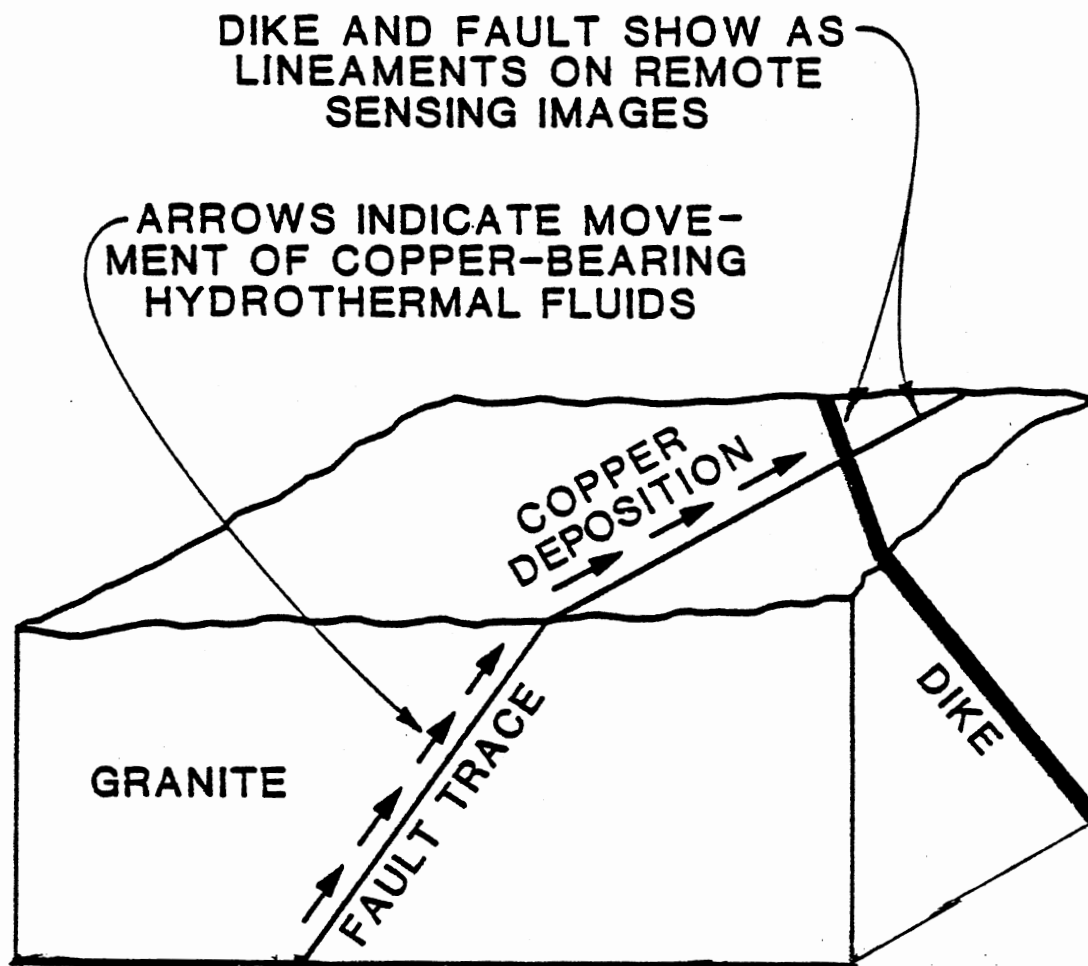


Figure 23. Conceptual Model of Ore Deposition

CHAPTER V

USE OF REMOTE SENSING TECHNIQUES

A. Background

The extrapolation of the Goldfield studies of Rowan et al. to the present study was hampered by the inability to obtain transparencies that reflected the results of the different band ratios. Instead, the results Rowan obtained were analyzed to determine the spectral characteristics of the altered rocks. In Rowan's final results, the altered rocks were either green or brown; the separate ratio colors were cyan for 4/5, green for 5/6, and magenta for 6/7. This was interpreted to mean that altered rocks had values high in the second and third and low in the first or of roughly equal value in all three. By this logic, pixel classes in the Sinai that show similar characteristics also may represent altered rocks.

The spectra of igneous rocks, as determined by Hunt, Salisbury, and Lenhoff (1973) support this conclusion only in a general way. Curves appear steeper for altered felsic rocks than for fresh granite, all specimens showing greater reflectance as wavelength increases. But, as the authors state, only a statistical breakdown would allow use of these spectral curves to be used as indicators of rock type. However, it is interesting to note the much steeper slope of the curve for kaolinite and montmorillonite (alteration products) as compared to orthoclase and plagioclase. Such steep curves could cause the ratios to appear as

discussed in the preceding paragraph.

Blodget, Gunther, and Podwyssocki (1978) remarked on the fact that altered rocks have a steep slope for the spectral reflectance curve between the green and red portions of the spectrum; this, they said, was due to the red, iron-rich rocks of the altered areas. They pointed out that such altered rocks thus have a lower value for the 4/5 ratio than the unaltered rocks.

Before applying Rowan's methods to this study, target areas within the igneous and metamorphic complex were chosen. These targets were chosen on the basis of work done by Nicolais (1976), who found metallic mineral deposits to be associated with lineament intersections, and on field work done in Sinai by the writer, who also found the Sinai copper deposits to be associated with lineament intersections. A flow sheet showing the process for the selection of the targets is shown as Figure 24. The target areas were then evaluated by methods derived from Rowan et al. (1974). The methods used are described below and are also shown as Figure 25.

B. Computer Processing of the Scene

A copy of the Landsat scene of southwest Sinai, in digital form on computer-compatible tape, was brought from Cairo to Oklahoma State University for certain processing that at the time could not be performed in Cairo. The tape was then manipulated at the Oklahoma State University Center for Applied Remote Sensing (CARS), using the ELAS program developed by NASA.

Geographical referencing was necessary to correct distortions caused by the rotation of the Earth while the satellite was acquiring the scene.

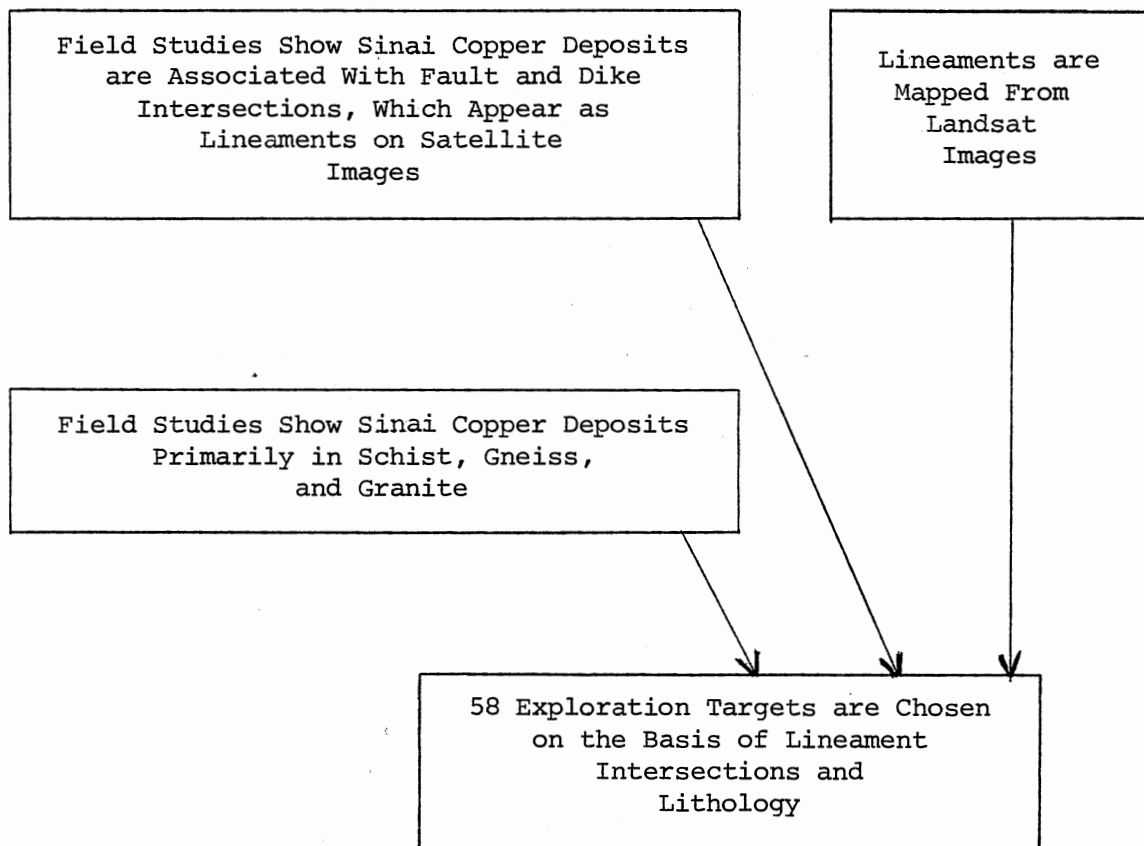


Figure 24. Geological Data Flow Chart

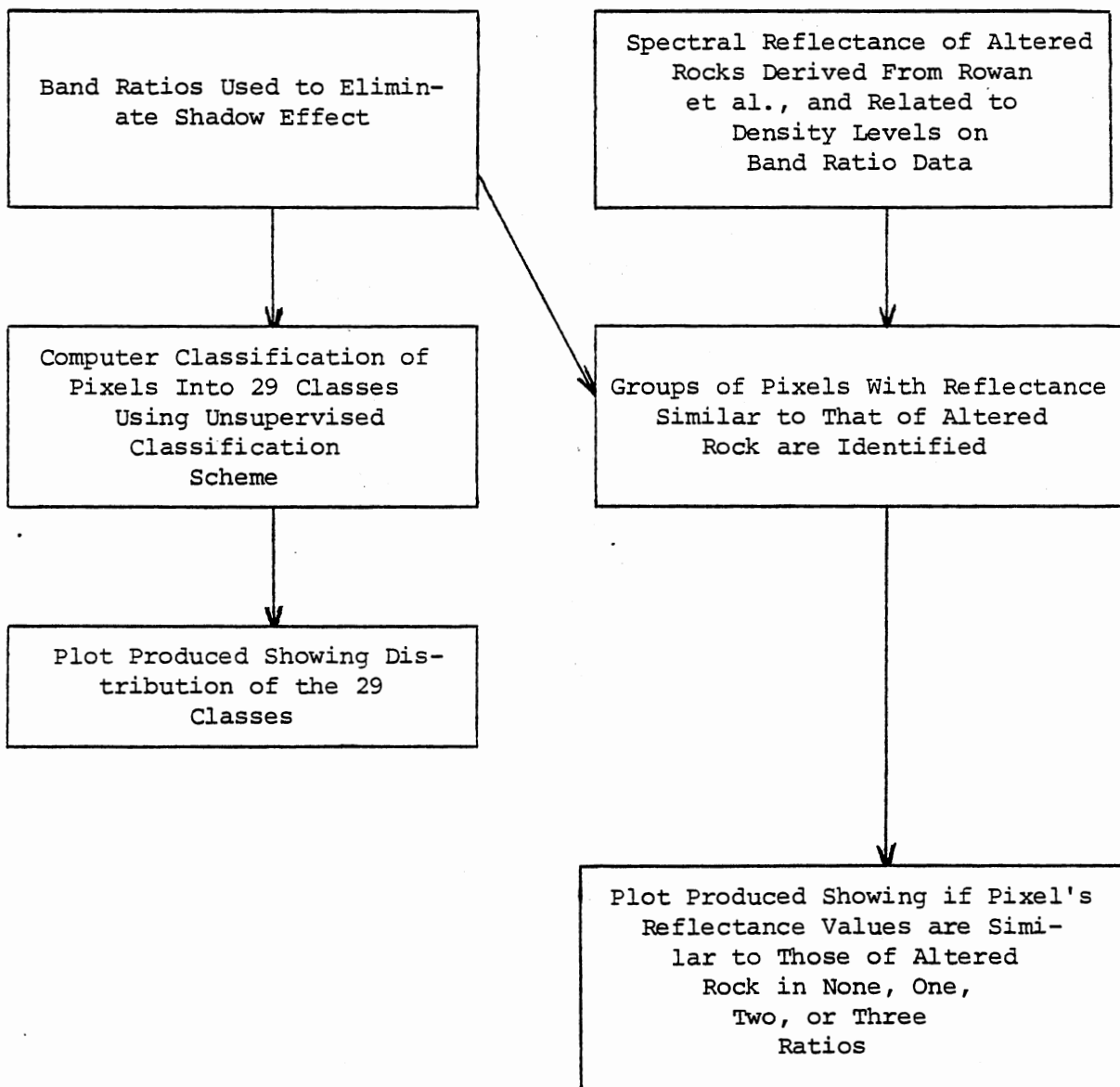


Figure 25. Computer Data Flow Chart

The process required use of a map on which the Universal Transverse Mercator grid appeared. The map selected for this purpose was the U.S. Army Map Service sheet designated "TOR"; numerical designation of this map was sheet NH 36-15 of the series P502. This map, published in 1958, was primarily a topographic map with wadis, springs, villages, and roads marked on the map. Comparison of the map with the satellite image and with maps published by the Remote Sensing Center in Cairo indicated that the Tor map was accurate along the coastline but might be inaccurate in the interior of the peninsula; the map itself stated that the information from which the map was derived was only "fair" in reliability. The points in the interior selected for georeferencing were mostly along wadis; some were wadi intersections, others were abrupt bends in the wadis. It was the subjective opinion of the writer that the wadis were accurately shown on the Tor map.

The GEOREF module of the ELAS program was used to correct image distortion. A number of points on the Tor map that could also be located with high degrees of accuracy on the satellite image were chosen. By means of a digital plotting table, the locations of the points in reference to the Universal Transverse Mercator Grid were determined. The computer used the resulting information to produce a corrected image; the error in determining specific point locations, however, meant that the averaging process used to produce the image placed the points in localities different from those fed into the computer. The points showing the greatest deviation were the points most likely to be misplotted while using the Tor map, and were eliminated one by one until the average error was under 50 meters. The resulting satellite image should thus show a point within 50 meters of its true location.

The satellite image that resulted based its accuracy on the accuracy of the Tor map and on the geographic spread of points used to correct the image; in other words, the points used would ideally be equally distributed over the entire area of the map and image. There was considerable difficulty involved in distributing the points in the desired manner. The image, however, agreed very well with the map along the coast of the Gulf of Suez, where the map had its highest degree of accuracy. The image was, therefore, accepted to be correct to a reasonable degree of accuracy.

The next step in the processing of the tape was to produce ratios of the reflectance values of each pixel in the different bands. This process, called band ratioing, was performed for two reasons. The first of the reasons is that the process minimizes effects caused by shadows; this is of considerable importance in the southern part of Sinai, it being a very mountainous region. The second reason is that the study performed by Rowan et al. in the Goldfield area found the method to be the most effective of the ones they evaluated in determining hydrothermally altered rocks. Following the lead of the Goldfield study, we used the ratios of bands 4/5, 5/6, and 6/7.

An unsupervised classification was performed on the results of the band ratioing. The unsupervised classification was considered to be better than a supervised classification because of the small amount of ground truth available. At the time of classification, the writer was unable to pinpoint areas of known lithology due to the unavailability of maps accurate enough to locate areas of known mineralization. The resulting classification performed by the computer used the principal maximum likelihood process and produced 29 classes; statistics on these

classes are in Tables I-V.

Certain lineament intersections had been designated as exploration targets earlier in the study based on work done by Nicolais (1976). The selection was based on field observations of mineralized localities and used lineament direction and areal lithology as prime criteria; density of lineament intersections was used as a secondary criterion. The target areas consisted of a circle around each intersection designated a target; the circle had a radius of one kilometer. An analysis was then made of the classes appearing in the circles and their frequency in the circles as compared to their frequency within the entire scene. The results of that analysis appear as Table II. Classes appearing in the target area with much greater or much lesser frequency than statistically predicted were of the most interest. Although several classes showed at least twice the expected frequency of occurrence, the outstanding class was class 22. This class comprised only 19.77 acres in the entire scene; of these 19.77 acres, 16.7 occurred within the targets! This class occurred 115 times more frequently in the target areas than expected. This class also had a spectral reflectance pattern (as shown in Table I) that was similar to that of hydrothermally altered rocks and was the only class to have such a pattern.

The results of the procedure described above can be summarized as follows. Fifty-eight target areas were selected on the basis of the lithology and structure; they resembled known hydrothermal deposits in Sinai in these two criteria. Each target area, centered on a lineament intersection, had a radius of one kilometer. The spectral reflectance values of these areas in 4 different ranges of the visible and near-infrared (photographic infrared) were ratioed and the resulting data

TABLE I
REFLECTANCE VALUE MEANS FOR BAND RATIO DATA

| Class | Points Measured | Ratio 4/5 | Ratio 5/6 | Ratio 6/7 |
|-------|-----------------|------------|--------------|-----------|
| 1 | 1416 | 44.90 | 55.51 | 124.97 |
| 2 | 103854 | 19.49 | 26.93 | 60.80 |
| 3 | 3335 | 51.42 | 48.27 | 124.99 |
| 4 | 950 | 52.21 | 35.50 | 254.70 |
| 5 | 137 | 53.38 | 47.09 | 61.94 |
| 6 | 227 | 48.56 | 33.07 | 200.11 |
| 7 | 1315 | 47.10 | 52.03 | 254.81 |
| 8 | 2196 | 48.74 | 42.76 | 254.93 |
| 9 | 210 | 51.33 | 40.35 | 75.03 |
| 10 | 455 | 44.61 | 40.44 | 175.11 |
| 11 | 310 | 44.97 | 46.34 | 75.00 |
| 12 | 223 | 53.06 | 42.34 | 175.45 |
| 13 | 546 | 56.86 | 43.58 | 254.89 |
| 14 | 4885 | 24.44 | 27.56 | 71.44 |
| 15 | 138 | 47.01 | 64.96 | 99.93 |
| 16 | 208 | 45.43 | 55.20 | 61.96 |
| 17 | 17993 | 22.31 | 28.31 | 63.19 |
| 18 | 234 | 28.35 | 30.05 | 92.39 |
| 19 | 1565 | 27.32 | 30.52 | 74.91 |
| 20 | 1390 | 27.31 | 30.63 | 62.39 |
| 21 | 123 | 39.63 | 36.26 | 192.89 |
| 22 | 161 | 47.34 | 62.29 | 252.08 |
| 23 | 428 | 33.17 | 31.10 | 86.05 |
| 24 | 148 | 34.57 | 33.98 | 117.55 |
| 25 | 410 | 29.28 | 27.08 | 69.13 |
| 26 | 336 | 32.10 | 31.19 | 70.88 |
| 27 | 20 | 19.55 | 27.30 | 30.16 |
| 28 | 102 | 36.91 | 61.78 | 249.71 |
| 29 | 38 | 60.92 | 36.87 | 181.58 |
| 1 | CHNS 3 | PTS = 1416 | APR = 3.5416 | |

TABLE II
 FREQUENCY OF CLASSES WITHIN THE TARGET AREAS

| Class | No. in Target Areas | Expected Frequency (No. of Pixels) | Actual Ratio/Expected Frequency |
|-------|---------------------|------------------------------------|---------------------------------|
| 1 | 1 | 0.14 | ----- |
| 2 | 0 | 0 | ----- |
| 3 | 9 | 4.8 | ----- |
| 4 | 4 | 5.5 | ----- |
| 5 | 2 | 0.7 | ----- |
| 6 | 0 | 3.0 | ----- |
| 7 | 0 | 1.2 | ----- |
| 8 | 0 | 3.95 | ----- |
| 9 | 0 | 1.3 | ----- |
| 10 | 0 | 2.5 | ----- |
| 11 | 5 | 1.5 | ----- |
| 12 | 0 | 0.9 | ----- |
| 13 | 0 | 0 | ----- |
| 14 | 1229 | 784.5 | 1.57 |
| 15 | 0 | 1.2 | ----- |
| 16 | 0 | 0.09 | ----- |
| 17 | 0 | 0 | ----- |
| 18 | 89 | 61.3 | 1.45 |
| 19 | 290 | 200 | 1.45 |
| 20 | 681 | 332.8 | 2.05 |
| 21 | 3 | 33.4 | .089 |
| 22 | 15 | 0.13 | 115.38 |
| 23 | 165 | 96.2 | 1.72 |
| 24 | 112 | 45.3 | 2.47 |
| 25 | 224 | 104 | 2.15 |
| 26 | 136 | 80.5 | 1.69 |
| 27 | 0 | 4.6 | ----- |
| 28 | 1 | 0.62 | ----- |
| 29 | 1 | 0.19 | ----- |

NOTE: Classes 2 and 17 not included in talley.

TABLE III
 FREQUENCY COUNTS - CLASSES OF BAND RATIOED SCENE

| Value | Freq. | Pct. | Acres | Sq. Mi. | Hect. |
|---|--------|--------|------------|---------|-----------|
| 1 | 9 | 0.000 | 22.24 | 0.03 | 9.00 |
| 2 | 842091 | 74.187 | 2080807.00 | 3251.26 | 842091.00 |
| 3 | 298 | 0.026 | 736.36 | 1.15 | 298.00 |
| 4 | 345 | 0.030 | 852.49 | 1.33 | 345.00 |
| 5 | 42 | 0.004 | 103.78 | 0.16 | 42.00 |
| 6 | 188 | 0.017 | 464.55 | 0.73 | 188.00 |
| 7 | 77 | 0.007 | 190.27 | 0.30 | 77.00 |
| 8 | 246 | 0.022 | 607.87 | 0.95 | 246.00 |
| 9 | 83 | 0.007 | 205.09 | 0.32 | 83.00 |
| 10 | 156 | 0.014 | 385.48 | 0.60 | 156.00 |
| 11 | 94 | 0.008 | 232.27 | 0.36 | 94.00 |
| 12 | 54 | 0.005 | 133.43 | 0.21 | 54.00 |
| 14 | 48875 | 4.306 | 120770.13 | 188.70 | 48875.00 |
| 15 | 67 | 0.006 | 165.56 | 0.26 | 67.00 |
| 16 | 6 | 0.000 | 14.83 | 0.02 | 6.00 |
| 17 | 182674 | 16.093 | 451387.38 | 705.29 | 182674.00 |
| 18 | 3822 | 0.337 | 9444.16 | 14.76 | 3822.00 |
| 19 | 12472 | 1.099 | 30818.31 | 48.15 | 12472.00 |
| 20 | 20731 | 1.826 | 51226.30 | 80.04 | 20731.00 |
| 21 | 2083 | 0.184 | 5147.09 | 8.04 | 2083.00 |
| 22 | 8 | 0.000 | 19.77 | 0.03 | 8.00 |
| 23 | 5995 | 0.528 | 14813.64 | 23.15 | 5995.00 |
| 24 | 2820 | 0.248 | 6968.22 | 10.89 | 2820.00 |
| 25 | 6503 | 0.573 | 16068.91 | 25.11 | 6503.00 |
| 26 | 5016 | 0.442 | 12394.54 | 19.37 | 5016.00 |
| 27 | 284 | 0.025 | 701.76 | 1.10 | 284.00 |
| 28 | 39 | 0.003 | 96.37 | 0.15 | 39.00 |
| 29 | 12 | 0.001 | 29.65 | 0.05 | 12.00 |
| TOTAL = 1135090 ACRES = 2804807.00 SQ MILES = 4382.51 | | | | | |
| HECT. = 1135090.00 | | | | | |

TABLE IV
TARGET CHARACTERIZATION

| Target | Lithology | Lineament Characteristics |
|--------|--|--|
| 1 | Acid metavolcanics, meta - tuffs | NNE lineament intersects cir- cular lineament |
| 2 | Same as #1 | Same as #1 |
| 3 | Pink granite, granodiorite | Triple intersection of NW, NE, and N-S lineaments |
| 4 | Same as #3 | NE and NW lineaments intersect |
| 5 | Same as #3 | Same as #4 |
| 6 | Same as #3 | Same as #4 |
| 7 | Same as #3 | NE and NW lineaments intersect; E-W lineament in junction vicinity |
| 8 | Same as #3 | Multiple intersections; NE, NW directions prominent |
| 9 | Same as #3 | NE, NW lineaments intersect |
| 10 | Gneiss, with granite contact nearby | NE, NW lineaments intersect |
| 11 | Granite, granodiorite | Multiple intersections |
| 12 | Same as #11 | Same as #11 |
| 13 | Pink granite, granodiorite | NE, NW lineaments intersect |
| 14 | Granodiorite | NW, NE lineaments intersect |
| 15 | Same as #14 | Same as #14 |
| 16 | Pink granite, granodiorite | Same as #14 |
| 17 | Same as #16 | Same as #14 |
| 18 | Pink granite, granodiorite | NE, NW lineaments intersect |
| 19-27 | Same as #18 | Same as #18 |
| 28 | Metatuff | NE, NW lineaments intersect |

TABLE IV (Continued)

| Target | Lithology | Lineament Characteristics |
|--------|---|-----------------------------|
| 31 | Contact of metatuff, granite, and granodiorite | Y - shaped intersection |
| 32 | Granodiorite | NE, NW lineaments intersect |
| 33 | Granodiorite | Multiple intersections |
| 34 | Granite | NE, NW lineaments intersect |
| 35 | Granite | NE, NW lineaments intersect |
| 36 | Granodiorite | NE, NW lineaments intersect |
| 37-39 | Granite | NE, NW lineaments intersect |
| 40 | Gneiss | NE, NW lineaments intersect |
| 41 | Gneiss | Multiple intersections |
| 42 | Gneiss | NE, NW lineaments intersect |
| 43 | Gneiss | Multiple intersections |
| 44 | Gneiss | NE, NW lineaments intersect |
| 45 | Same as #44 | Same as #44 |
| 46 | Gneiss/granite contact | NE, NW lineaments intersect |
| 47-49 | Porphyritic granite | NE, NW lineaments intersect |
| 50-51 | Granite, granodiorite | NE, NW lineaments intersect |
| 52 | White granite | NE, NW lineaments intersect |
| 53 | Pink granite, granodiorite | Same as #52 |
| 54 | Porphyritic pink granite | Multiple intersections |
| 55 | Pink granite, granodiorite | NE, NW lineaments intersect |
| 56 | Same as #55 | Multiple intersections |
| 57-58 | Pink granite, granodiorite | NW, NE lineaments intersect |

TABLE V
PIXEL CLASS FREQUENCY IN TARGET AREAS

| TARGET AREA | PIXEL CLASS | | | | | | | | | | | | | | | | | | | | | | | | | | | | | | | | | | | | | | |
|-------------|-------------|---|---|---|---|---|---|---|---|----|----|----|----|----|----|----|----|----|----|----|----|----|----|----|----|----|----|----|----|---|---|---|---|--|--|--|--|--|--|
| | 1 | 2 | 3 | 4 | 5 | 6 | 7 | 8 | 9 | 10 | 11 | 12 | 13 | 14 | 15 | 16 | 17 | 18 | 19 | 20 | 21 | 22 | 23 | 24 | 25 | 26 | 27 | 28 | 29 | | | | | | | | | | |
| 1 | | | | | | | | | | | | | 23 | | | | | | 1 | 8 | | | | | | | | | | 4 | | | | | | | | | |
| 2 | | | | | | | | | | | | | 2 | | | | | | | | | | | | | | | | | 1 | | | | | | | | | |
| 3 | | | | | | | | | | | | | 12 | | | | | | | | | | | | | | | | | 1 | | | | | | | | | |
| 4 | | | | | | | | | | | | | | | | | | | | | | | | | | | | | | 3 | | | | | | | | | |
| 5 | | | | | | | | | | | | | | 31 | | | | 2 | 3 | 10 | | | | 1 | 3 | 5 | 3 | | | 3 | | | | | | | | | |
| 6 | | | | | | | | | | | | | 13 | | | | | | 3 | 4 | | | | | | | | | | | | | | | | | | | |
| 7 | | | | | | | | | | | | | 14 | | | | | | 1 | 1 | 12 | | | 1 | | 1 | | | | | | | | | | | | | |
| 8 | | | | 2 | | | | | | | | | 23 | | | | | | 3 | 11 | 11 | 4 | | 8 | 3 | 5 | 3 | | | | | | | | | | | | |
| 9 | | | | | | | | | | | | | 16 | | | | | | 1 | 1 | 2 | | | 2 | | 2 | 1 | | | | | | | | | | | | |
| 10 | | | | | | | | | | | | | | | | | | | | | | | | | | | | | | | | | | | | | | | |
| 11 | | | | 1 | | | | | | | | | 23 | | | | | | 2 | 12 | 27 | 1 | | 12 | 8 | 9 | 7 | | | | | | | | | | | | |
| 12 | 1 | | | 1 | | | | | | | 3 | | 23 | | | | 28 | 2 | 10 | 11 | | | 5 | 1 | 5 | 11 | | | | | | | | | | | | | |
| 13 | | | | | | | | | | | | | 16 | | | | | | 3 | 5 | | | | | | | | | | | | | | | | | | | |
| 14 | | | | | | | | | | | | | 11 | | | | | | 1 | 3 | 8 | | | | | | | | | | 5 | 2 | | | | | | | |
| 15 | | | | | | | | | | | | | 41 | | | | | | 1 | 16 | | | | | 1 | 4 | 2 | | | | | | | | | | | | |
| 16 | | | | | | | | | | | | | 31 | | | | | | 2 | 4 | 14 | | | | | | | | | | | | | | | | | | |
| 17 | | | | | | | | | | | | | 27 | | | | | | 4 | 21 | 23 | | | 12 | 5 | 7 | 14 | | | | | | | | | | | | |
| 18 | | | | 1 | 1 | 1 | 1 | | | | 1 | | 23 | | | | | | 3 | 9 | 10 | 7 | | 13 | 6 | 3 | 5 | | | | | | 1 | | | | | | |
| 19 | | | | 3 | 1 | 1 | 1 | | | | 1 | | 13 | | | | | | 2 | 5 | 6 | | 15 | 11 | 11 | 1 | 8 | | | | | | 1 | | | | | | |
| 20 | | | | | | | | | | | | | 26 | | | | | | | 7 | 8 | | | | 1 | 4 | 5 | 2 | | | | | | | | | | | |
| 21 | | | | 1 | | | | | | | 1 | 2 | 14 | | | | | | 3 | 7 | 20 | 10 | | 10 | 8 | 6 | 6 | | | | | | | | | | | | |
| 22 | | | | 2 | | | | | | | | | 13 | | | | | | 2 | 6 | 10 | 8 | | 5 | 9 | 17 | 4 | | | | | | | | | | | | |
| 23 | | | | | | | | | | | | | 34 | | | | | | 4 | 4 | 17 | 1 | | 3 | 2 | 7 | 6 | | | | | | | | | | | | |
| 24 | | | | | | | | | | | | | 19 | | | | | | | 3 | 11 | | | 2 | 1 | 8 | 5 | | | | | | | | | | | | |
| 25 | | | | | | | | | | | | | 15 | | | | | | 1 | 2 | 8 | | | 2 | | 1 | | | | | | | | | | | | | |
| 26 | | | | | | | | | | | | | 9 | | | | | | | | | | | | | | | | | | | | | | | | | | |
| 27 | | | | | | | | | | | | | 2 | | | | | | | | | | | | | | | | | | | | | | | | | | |
| 28 | | | | | | | | | | | | | 5 | | | | | | | | | | | | | | | | | | | | | | | | | | |
| 29 | | | | | | | | | | | | | 66 | | | | | | | 3 | 6 | 26 | | | | | | | | | | | | | | | | | |
| 30 | | | | | | | | | | | | | 21 | | | | | | | | 6 | 6 | | | | | | | | | | | | | | | | | |
| 31 | | | | | | | | | | | | | | | | | | | 1 | 10 | 3 | | | | | | | | | | | | | | | | | | |
| 32 | | | | | | | | | | | | | 34 | | | | | | | 1 | 4 | 21 | | | | 1 | 3 | | | | | | | | | | | | |
| 33 | | | | | | | | | | | | | 27 | | | | | | | | 10 | 10 | | | 1 | 2 | 2 | 2 | | | | | | | | | | | |
| 34 | | | | | | | | | | | | | 48 | | | | | | | 6 | 9 | 19 | | | | | | | | | | | | | | | | | |
| 35 | | | | | | | | | | | | | 36 | | | | | | | 3 | 11 | 20 | | | 4 | 1 | 6 | | | | | | | | | | | | |
| 36 | | | | | | | | | | | | | 23 | | | | | | | | 1 | | | | 1 | 1 | 1 | | | | | | | | | | | | |
| 37 | | | | | | | | | | | | | 34 | | | | | | | 4 | 7 | 19 | | | | | 6 | 4 | | | | | | | | | | | |
| 38 | | | | | | | | | | | | | 10 | | | | | | | 2 | 3 | 4 | | | | | 2 | | | | | | | | | | | | |
| 39 | | | | | | | | | | | | | 40 | | | | | | | | | 19 | | | | | 4 | 3 | | | | | | | | | | | |
| 40 | | | | | | | | | | | | | 15 | | | | | | | 1 | 10 | | | | | | 1 | | | | | | | | | | | | |
| 41 | | | | | | | | | | | | | 2 | | | | | | | | | | | | | | | | | | | | | | | | | | |
| 42 | | | | | | | | | | | | | 13 | | | | | | | | | | | | | | | | | | | | | | | | | | |
| 43 | | | | | | | | | | | | | 17 | | | | | | | 1 | 3 | | | | 1 | | | | | | | | | | | | | | |
| 44 | | | | | | | | | | | | | 4 | | | | | | | 5 | 14 | 18 | | | 3 | 2 | 12 | 6 | | | | | | | | | | | |
| 45 | | | | | | | | | | | | | 29 | | | | | | | | 10 | | | | 3 | 5 | 2 | | | | | | | | | | | | |
| 46 | | | | | | | | | | | | | 18 | | | | | | | 2 | 4 | 16 | | | 4 | 7 | 2 | 6 | | | | | | | | | | | |
| 47 | | | | 1 | 7 | | 1 | | | | | | 17 | | | | | | | 2 | 2 | 5 | | | 4 | | 3 | | | | | | | | | | | | |
| 48 | | | | | | | | | | | | | 27 | | | | | | | 7 | 11 | 15 | 2 | | 12 | 7 | 11 | 10 | | | | | | | | | | | |
| 49 | | | | | | | | | | | | | 27 | | | | | | | 5 | 15 | 20 | | | 5 | 1 | 7 | 6 | | | | | | | | | | | |
| 50 | | | | | | | | | | | | | 26 | | | | | | | 11 | 11 | 36 | 3 | | 17 | 18 | 15 | 10 | | | | | | | | | | | |
| 51 | | | | | | | | | | | | | 26 | | | | | | | 4 | 8 | 10 | 1 | | | | 2 | 4 | | | | | | | | | | | |
| 52 | | | | | | | | | | | | | 13 | | | | | | | | 2 | 6 | | | 3 | | | | | | | | | | | | | | |
| 53 | | | | | | | | | | | | | 15 | | | | | | | 7 | 11 | 1 | | | 10 | 4 | 5 | 5 | | | | | | | | | | | |
| 54 | | | | | | | | | | | | | 31 | | | | | | | 3 | 13 | 7 | 3 | | 30 | 8 | 7 | 5 | | | | | | | | | | | |
| 55 | | | | | | | | | | | | | 7 | | | | | | | | 1 | | | | | | | | | | | | | | | | | | |
| 56 | | | | | | | | | | | | | 6 | | | | | | | 3 | 1 | | | | | | | | | | | | | | | | | | |
| 57 | | | | | | | | | | | | | 51 | | | | | | | 3 | 16 | 40 | | | 4 | 10 | 3 | | | | | | | | | | | | |
| 58 | | | | | | | | | | | | | 24 | | | | | | | | | | | | | | | | | | | | | | | | | | |

* Not analyzed due to their forming the most common classes (see Table III).

were statistically grouped into 29 classes. One and only one class displayed a spectral reflectance pattern similar to that of hydrothermally altered rocks; the same class was the only one that occurred in the target areas with a frequency much greater than random distribution would allow. Sections of the resulting plots are seen in Appendix I.

A second procedure was used to attempt to locate areas of hydrothermal alteration. This method is also based on the fact that altered rocks have different reflectance values from those of unaltered rocks. Again, band ratio data were used. The reflectance values for minerals associated with hydrothermal alteration were obtained from U.S. Geological Survey Professional Paper 883. The values (V) given in that publication had to be converted to the value levels obtained when the Sinai image was processed at the OSU Remote Sensing Center. The formula used for conversion was

$$\frac{V - \text{min}}{\text{max} - \text{min}} \quad (127)$$

where:

- V = Reflectance values from Professional Paper 883
- min = Minimum value in the band ratio
- max = Maximum value in the band ratio

For band ratios 4/5 and 5/6, V was first multiplied by 25; for ratio 6/7, it was multiplied by 50. This manipulation was necessary to allow for the fact that band 7 has 63 levels of density, as opposed to 127 for the other bands.

The density levels thus obtained were then assembled into three groups, one for each band ratio. The groups were then used to generate

a plot showing which pixels had reflectance values in one or more of the groups. A single dot was used to represent pixel with a reflectance value falling into the selected group in one band ratio. If the pixel had the desired reflectance values in two band ratios, a diagonal line was plotted for that pixel. If the pixel's reflectance value in all three ratios fell into the target groups, a totally black pattern was used for the pixel. Sections of the resulting plot are shown in Figures 21 and 22.

Only 0.008% of the image showed the all-black pattern; none of the 94 pixels in that group was in a target. There are concentrations at 3 places in the igneous-metamorphic complex. On the grid used in this report, these are:

| | |
|---------|--------|
| 87.25E, | 66.93N |
| 90.10E, | 66.85N |
| 89.90E, | 63.55N |

These do not coincide with lineament intersections, nor with the location of Regeita.

Three lineament intersections chosen as targets were within 1' of latitude and longitude of known copper deposits. These three were:

| |
|-------------------|
| #3 - Rahaba |
| #36 - Zagatan |
| #45 - Abu Suweira |

However, El Tarr, located at $33^{\circ} 38' 20''$ E, $28^{\circ} 43' 38''$ N, and Abu El Nimran, at $33^{\circ} 34' 17''$ E, $28^{\circ} 49' 46''$ N, are known copper deposits but were not located at lineament intersections chosen as targets.

C. Photographic Techniques

Although aerial photographs would possibly have been of use in the study, especially when large-scale, they were unavailable. Hand-held cameras were used to take photographs of areas visited during field investigations, however. Agfachrome 100 color slide film was used in one camera, while in another Ektachrome infrared color slide film was used in conjunction with a yellow filter. The ASA of the infrared film was estimated to be approximately 250, which was halved by use of the filter; the f-stop was set at 11 and the automatic light meter was used to determine exposure time.

One interesting phenomenon was noted in the infrared photographs of the Regeita area; mineralized areas, which were blue in the photographs, were extremely prominent compared to visible-light photographs. Since the exposure times were bracketed, it was possible to determine that a slightly over-exposed photographs showed the phenomenon to a larger degree than under-exposed or normally-exposed ones. In light of this finding, a high-altitude color infrared photograph of a porphyry copper mine in New Mexico was obtained. The tailings, which should contain copper minerals similar to the ones found in Sinai, were distinctly blue on the photograph.

CHAPTER VI

CONCLUSIONS

Based on mineral texture and the minerals present, the copper deposits examined by the writer in Sinai were formed by hydrothermal processes in the epithermal range. Primary sulfides replaced pre-existing mineral grains and were in turn altered. The deposits are associated with faults (probably the conduits for the hydrothermal fluids) and with aphanitic dikes.

The fifty-eight exploration targets were chosen from a Landsat image on the basis of lineament intersections and the lithology at the intersections. In addition, at least 3 of these targets were found to coincide with known copper deposits. These targets were analyzed to determine if any of them showed evidence of hydrothermal alteration. The spectral reflectance pattern of one of the 29 populations of pixels was similar to that of hydrothermally altered rocks. Fifteen of the seventeen pixels in this population were in target 19. On the basis of this evidence, it is concluded that this target area has been hydrothermally altered.

The Regeita deposit as plotted did not fall within one of the 58 selected targets, nor was it represented by the alteration class (#22) derived from the computer analyses. The probable reasons for this failure are threefold: the exact location of Regeita could not be obtained; its location could be several kilometers from where it was plotted. The

structural features involved at Regeita are probably too small to be prominent at the scale we used to map lineaments. Finally, alteration at the deposit was not obvious in the field. Finer resolution might detect this deposit, at least as a target area.

CHAPTER VII

RECOMMENDATIONS

Further evaluation of the exploration targets should include inspection in the field by geologists. Signs of mineralization or hydrothermal alteration should be searched for in these areas. Special attention should be given to faults, which apparently act in this region as conduits for ore-bearing fluids.

Target area No. 19 should have the highest priority, due to its concentration of pixels having a reflectance pattern similar to that of hydrothermally altered rocks. There are no criteria to determine which of the other target areas are the most promising.

Airborne investigations may prove useful in evaluation of the targets. Many, but not all, metallic ore bodies show as positive anomalies when gravimeters and magnetometers are used. Aerial photography may also prove useful; color photography might show areas of alteration, while black and white photography could enable an investigator to locate faults. The photographs would be most effective if they were large-scale, at least 1:20,000.

A second attempt to locate altered areas involved the selection of pixels whose spectral reflectance in all three band ratios was similar to that of altered rock. None of the 94 pixels so selected were within a target; there were, however, linear concentrations that might represent alteration along faults (see Appendix B, Figures 40 and 41).

BIBLIOGRAPHY

- Aarnisalo, J., 1978, Use of Satellite Pictures for Determining Major Shield Fractures Relevant for Ore Prospecting, Northern Finland; Geological Survey of Finland, Report of Investigation 21.
- Anderson, A. T., and Smith, A. F., 1975, Application of LANDSAT Imagery to Metallic Mineral Exploration in Utah. Am. Soc. Photogramm., Fall Conv., Proc., Vol. 1975, pp. 286-297.
- Ball, J., 1916, The Geography and Geology of West Central Sinai. Survey Dept. of Egypt, Cairo, Egypt.
- Barron, T., 1907, The Topography and Geology of the Peninsula of Sinai (Western Portion). Survey Dept. of Egypt, Cairo, Egypt.
- Blodget, H. W., Gunther, F. J., and Podwysocki, H., 1978, Discrimination of Rock Classes and Alteration Products in Southwestern Saudi Arabia With Computer-Enhanced LANDSAT Data: NASA Technical Paper 1327.
- Davey, J. C., 1948, Report on Southern Sinai: Mining Mag., London, Vol. 78, No. 4, pp. 212-214.
- Degens, E. T., and Ross, David A., (editors), 1969, Hot Brines and Recent Heavy Metal Deposits in the Red Sea: Springer Verlag, New York.
- El Shazly, E. M., Abdel Naser, S., and Shukri, B., 1955, Contribution to the Mineralogy of the Copper Deposits in Sinai. Geological Survey of Egypt, Paper No. 1, Cairo, Egypt.
- El Shazly, E. M., et al., 1979, Geology of Sinai Peninsula From ERTS-1 Satellite Images: The Remote Sensing Research Project, Academy of Scientific Research and Technology, Cairo, Egypt.
- Garson, M. S. and Krs, M., 1976, Geophysical and Geological Evidence of the Relationship of Red Sea Transverse Tectonics to Ancient Fractures: Geological Society of America, Bulletin, Vol. 87, pp. 169-181.
- Hilmy, M. E., and Mohsen, L. A., 1966, Geology of Some Occurrences of Copper Minerals in Sinai: Ain Shams Science Bulletin (Cairo), Vol. 9, pp. 517-539.

- Hilmy, M. E., and Mohsen, L. A., 1965, Secondary Copper Minerals From West Central Sinai: *Journ. Geology, U.A.R.*, pp. 1-12.
- Hume, W. F., 1909, The Topography and Geology of the Peninsula of Sinai (South Eastern Portion). Survey Dept. of Egypt, Cairo, Egypt.
- Hunt, G. R., 1977, Spectral Signatures of Particulate Minerals in the Visible and Near Infrared: *Geophysics*, Vol. 42, pp. 501-513.
- Hunt, G. R., and Salisbury, J. W., 1970, Visible and Near-Infrared Spectra of Minerals and Rocks: I. Silicate Minerals: *Modern Geology*, Vol. 1, pp. 283-300.
- Hunt, G. R., Salisbury, J. W., and Lenhoff, C. J., 1973, Visible and Near-Infrared Spectra of Minerals and Rocks: VI. Additional Silicates: *Modern Geology*, Vol. 4, pp. 85-106.
- Hunt, G. R., Salisbury, J. W., and Lenhoff, C. J., 1973, Visible and Near Infrared Spectra of Minerals and Rocks: VII. Acidic Igneous Rocks: *Modern Geology*, Vol. 9, pp. 217-224.
- Moore, J., 1976, A Major Lineament in the Arabian Shield and its Relationship to Mineralization: *Mineralium Deposita*, Vol. 11, pp. 323-328.
- Nathan, Y., Bentor, Y. K., and Wurzbarger, V., 1970, Vein Palygorskites in Israel and Sinai, Their Origin and Symmetry: *Israeli Journal of Chemistry*, Vol. 8, No. 3, pp. 469-476.
- Nicolais, S., 1976, Mineral Exploration With ERTS Imagery: *NASA Special Publication 351*, 1974, pp. 785-796.
- O'Driscoll, E. S. T., 1981, Structural Corridors in Landsat Lineament Interpretation: *Mineralium Deposita*, Vol. 16, pp. 85-101.
- Offield, T. W., et al., 1977, Structure Mapping on Enhanced Landsat Images of Southern Brazil: Tectonic Control of Mineralization and Speculations on Metallogeny: *Geophysics*, Vol. 42, pp. 482-500.
- Raines, G. L., 1978, Porphyry Copper Exploration Model for Northern Sonora, Mexico: *Jour. Research U.S. Geol. Survey*, Vol. 6, pp. 51-58.
- Rowan, L. C., et al., 1976, Discrimination of Rock Types and Detection of Hydrothermally Altered Areas in South-Central Nevada by the Use of Computer-Enhanced ERTS Images: *U.S. Geol. Surv. Prof. Paper 883*.
- Ramos, V. A., 1977, Basement Tectonics From Landsat Imagery in Mining Exploration: *Geologic En Mijnbouw*, Vol. 56, pp. 243-252.
- Robson, D. A., 1971, The Structure of the Gulf Suez (Clysmic Rift) With Special Reference to the Eastern Side. *Journ. of Geological Society of London*, Vol. 127, pp. 247-277.

- Schmidt, R. G., 1976, Exploration for Porphyry Copper Deposits in Pakistan Using Digital Processing of Landsat-1 Data: Jour. Research U.S. Geol. Surv., Vol. 4, pp. 27-34.
- Schurmann, H. M. E., 1966, The Pre-Cambrian Along the Gulf of Suez and the Northern Part of the Red Sea: E. J. Brill, Leiden, The Netherlands.
- Siednet, G., Shimron, A. E., and Pringle, J. R., 1974, Age Relationships in Basement Rocks of the Sinai Peninsula: International Meeting for Geochronology, Cosmochronology, and Isotope Geology, Paris.
- Sheta, Abd-El-Fatah Ibrahim, 1969, Geology of Sherm El-Sheikh Area With Special Reference to Kaolinitic Deposits and Other Deposits: Unpublished Thesis, Ain Shams University, Cairo, Egypt.
- Shimron, Aryeh E., 1980, Proterozoic Island Arc Volcanism and Sedimentation in Sinai: Precambrian Research, Vol. 12, pp. 437-458.
- Soliman, S. M., and El Fetouh, M. A., 1969, Petrology of the Carboniferous Sandstones in West Central Sinai, Journal of Geology of the U.A.R., Vol. 13(2), pp. 61-143.
- Wachs, D., Arad, A., and Olshina, A., 1979, Locating Groundwater in the Santa Catherina Area Using Geophysical Methods: Groundwater, Vol. 17, No. 3, pp. 258-263.
- Weissbrod, T., 1969, The Paleozoic of Israel and Adjacent Countries, Part II, The Paleozoic Outcrops in Southwestern Sinai and Their Correlation With Those of Southern Israel: Geological Survey of Israel Bull. 48.

APPENDIX A

LINEAMENT MAPS

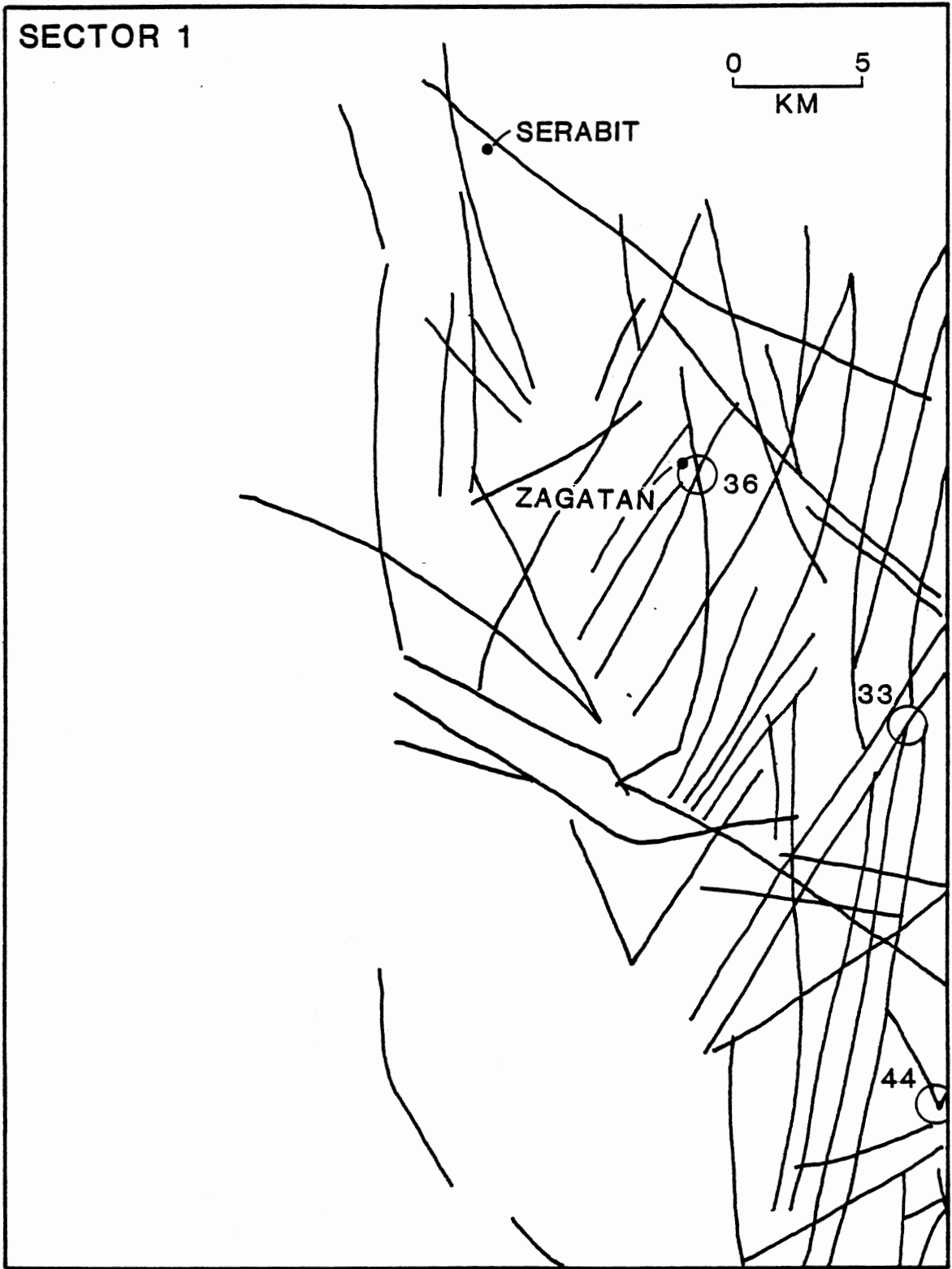


Figure 26. Lineament Map, Sector 1 (See Figure 4 for Index)

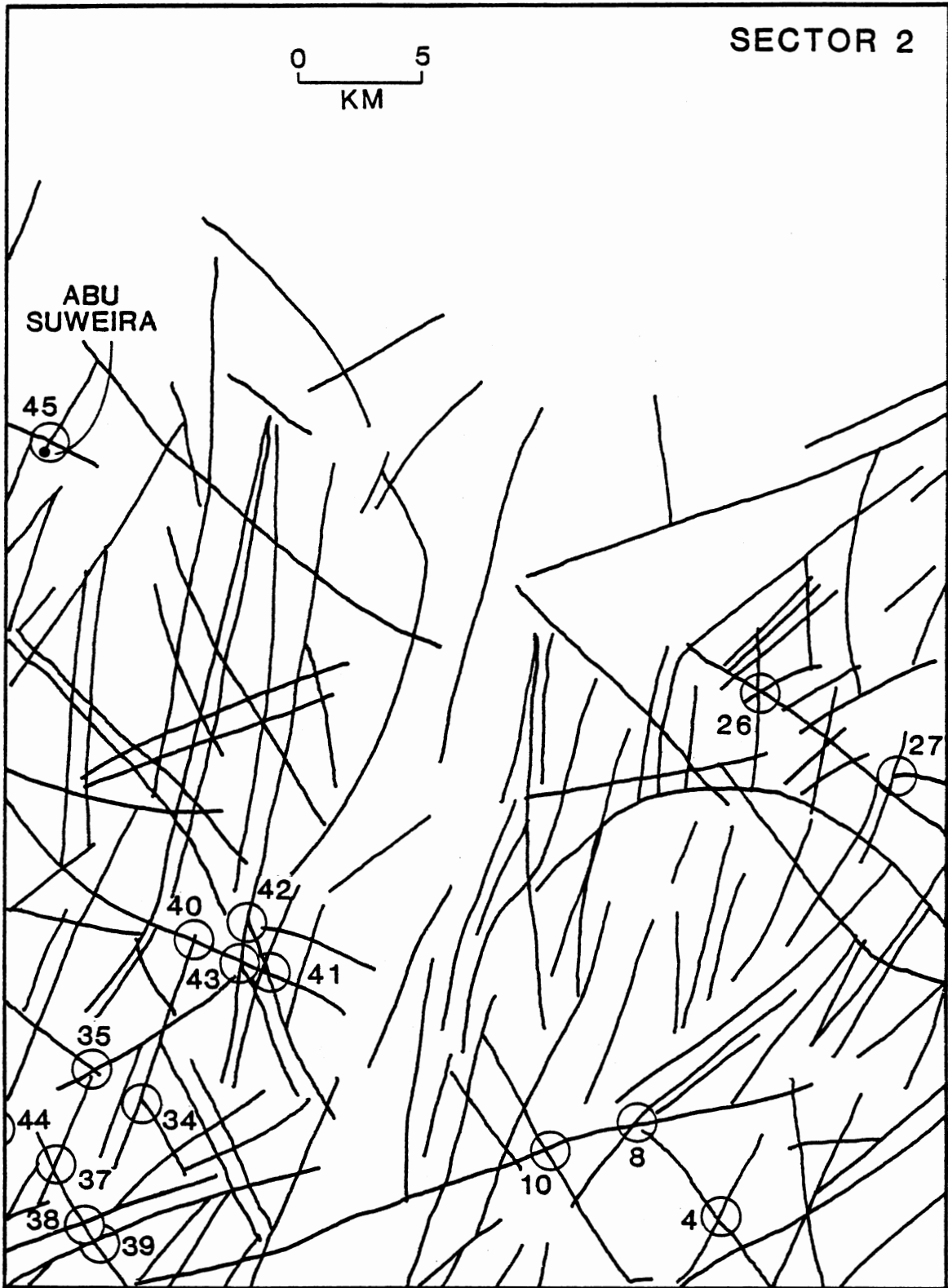


Figure 27. Lineament Map, Sector 2 (See Figure 5 for Index)

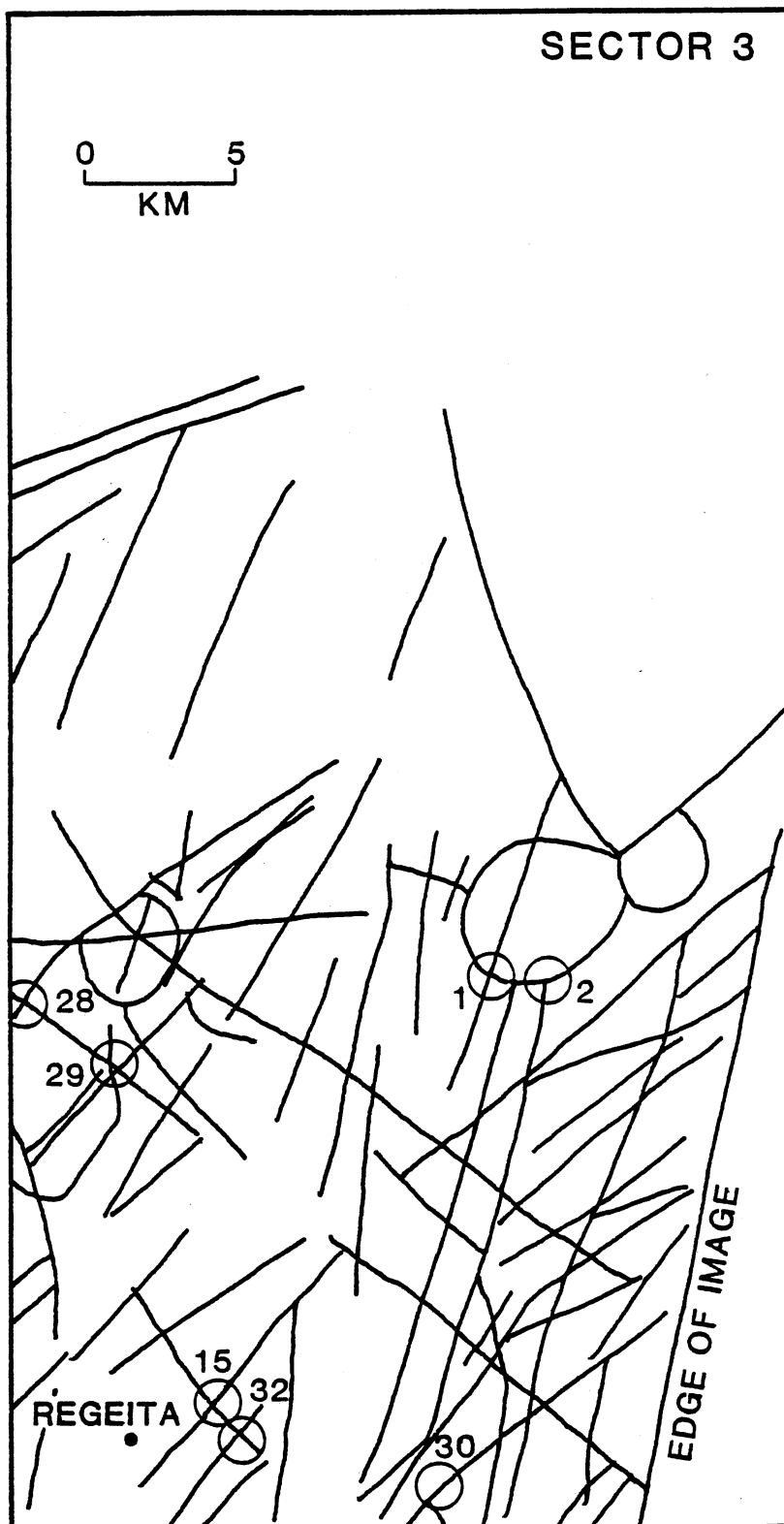


Figure 28. Lineament Map, Sector 3 (See Figure 5 for Index)

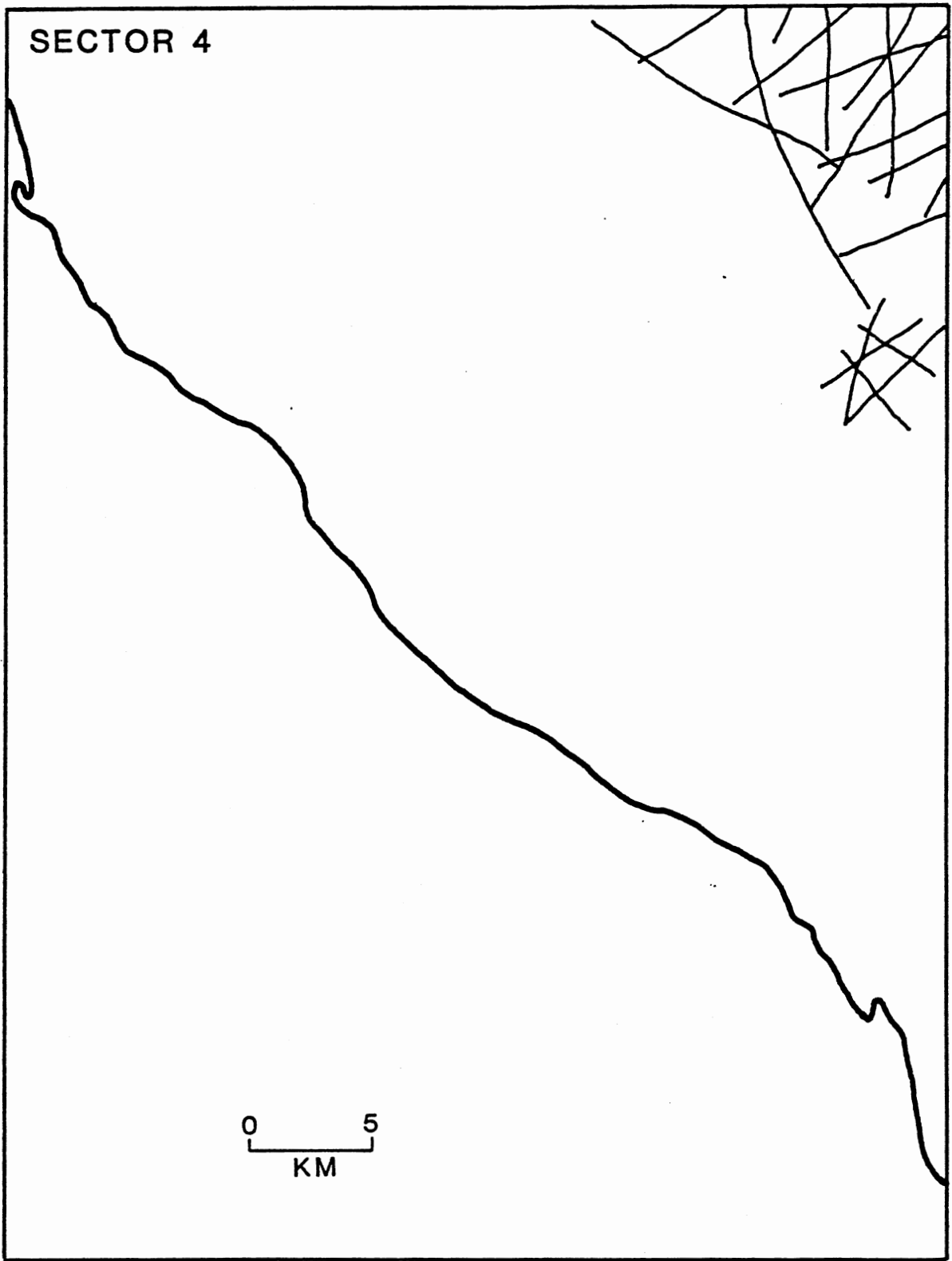


Figure 29. Lineament Map, Sector 4 (See Figure 5 for Index)

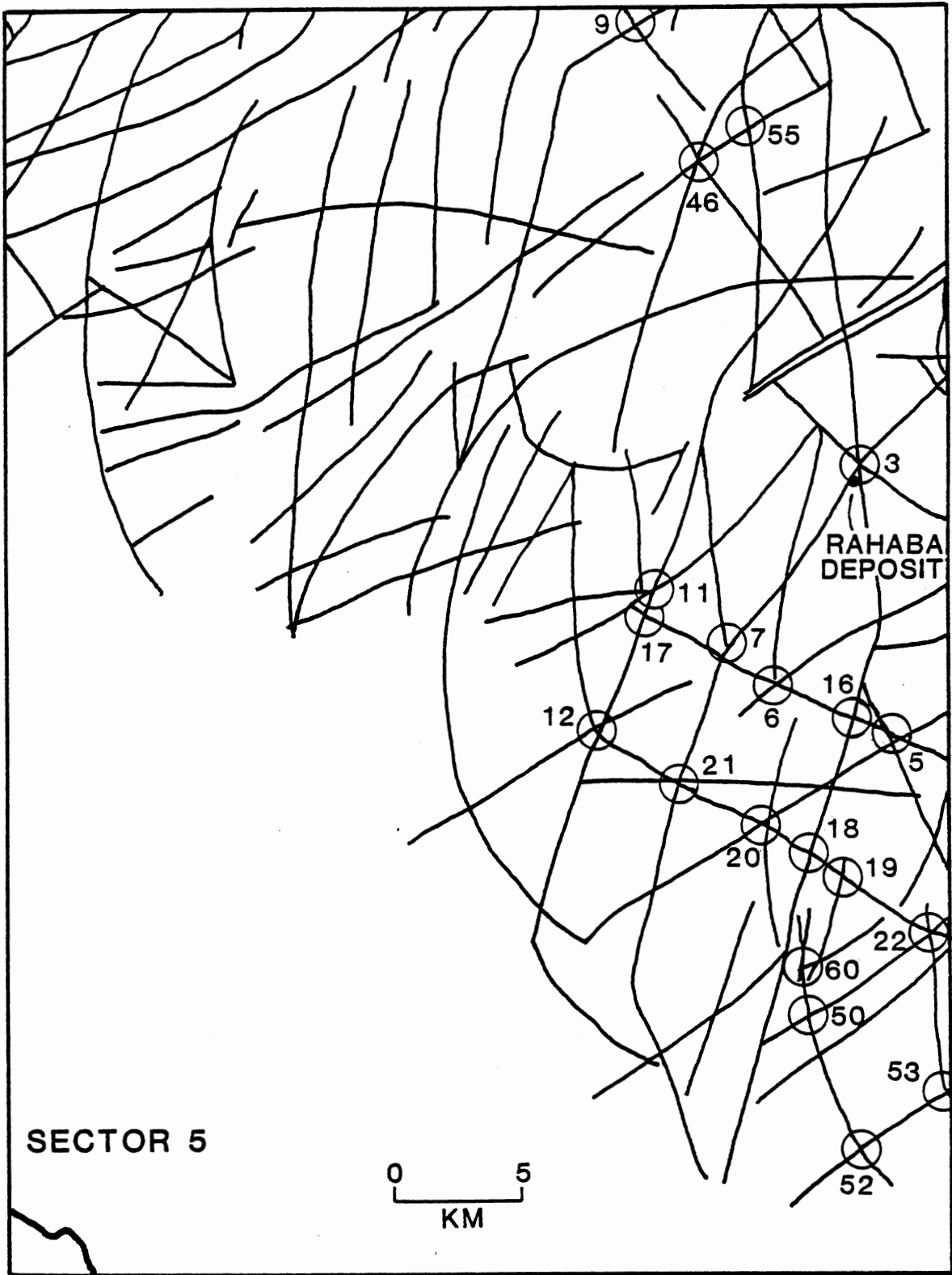


Figure 30. Lineament Map, Sector 5 (See Figure 5 for Index)

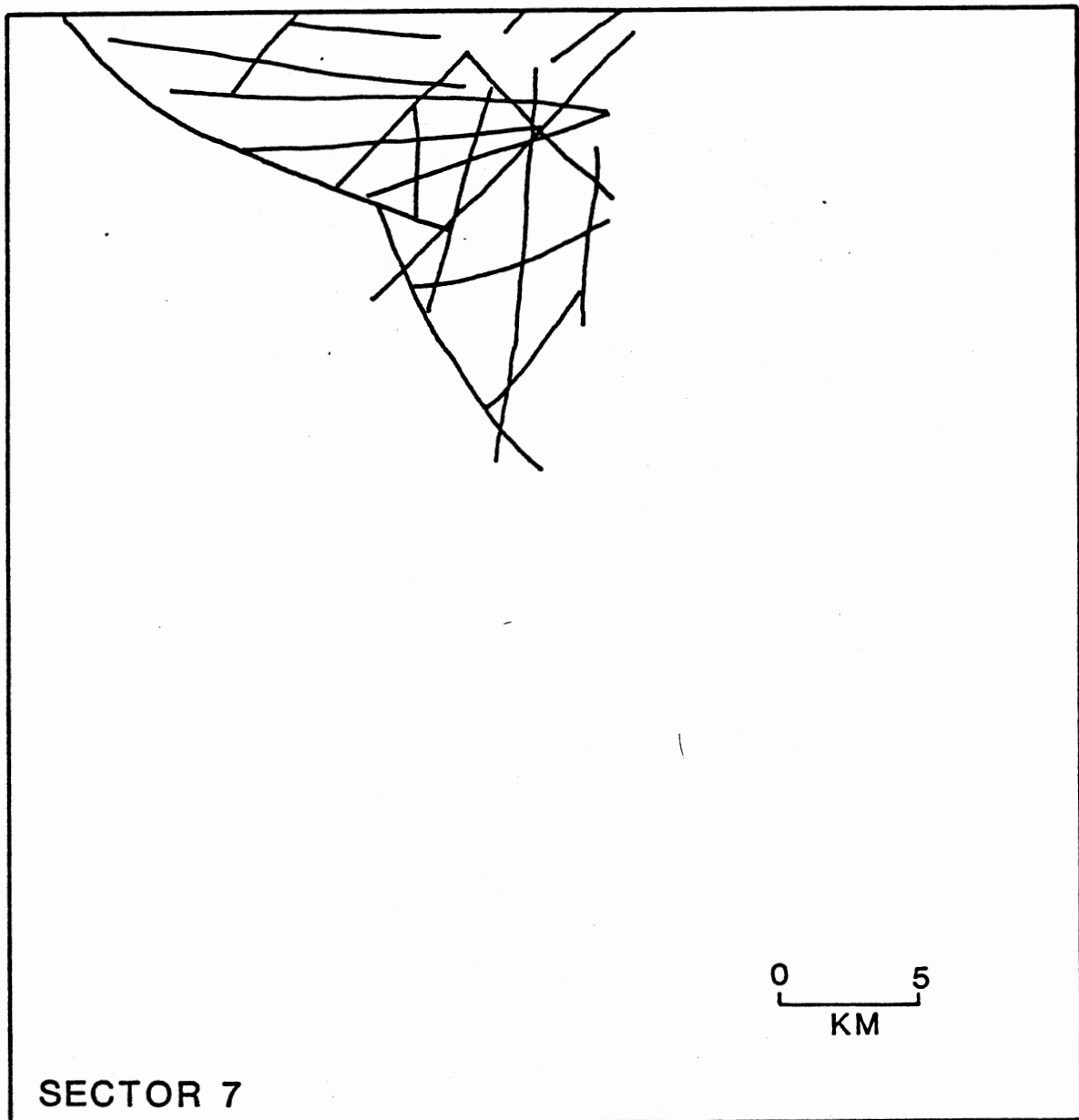


Figure 32. Lineament Map, Sector 7 (See Figure 5 for Index)

APPENDIX B

BAND RATIO CLASSIFICATION PLOTS OF
SELECTED AREAS

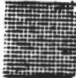
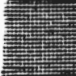







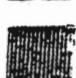
| | File 1 | File 2 | File 3 |
|---|--------|--------|--------|
|  | 4 | 2 | 20 |
|  | 6 | | 21 |
|  | 7 | 17 | 22 |
|  | 8 | 9 | 23 |
|  | 10 | 16 | 24 |
|  | 12 | 1 | 25 |
|  | 14 | 3 | 26 |
|  | 13 | 5 | 27 |
|  | 18 | 15 | 28 |
|  | 19 | 11 | 29 |

Figure 33. Symbols Used for Band Ratio Plots

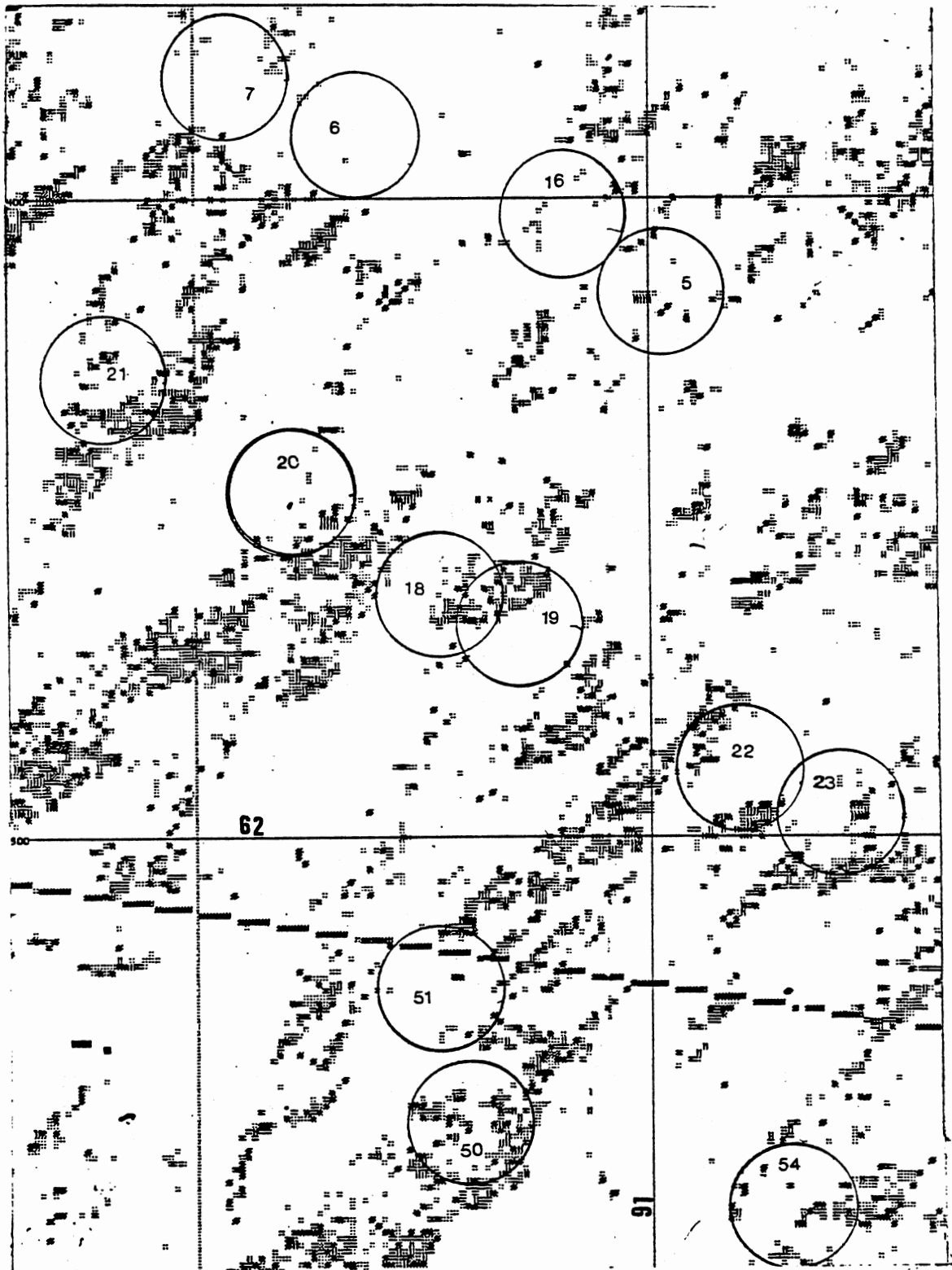


Figure 34. Target 19, Band Ratio Classification, File 1, Scale 1:98,
425

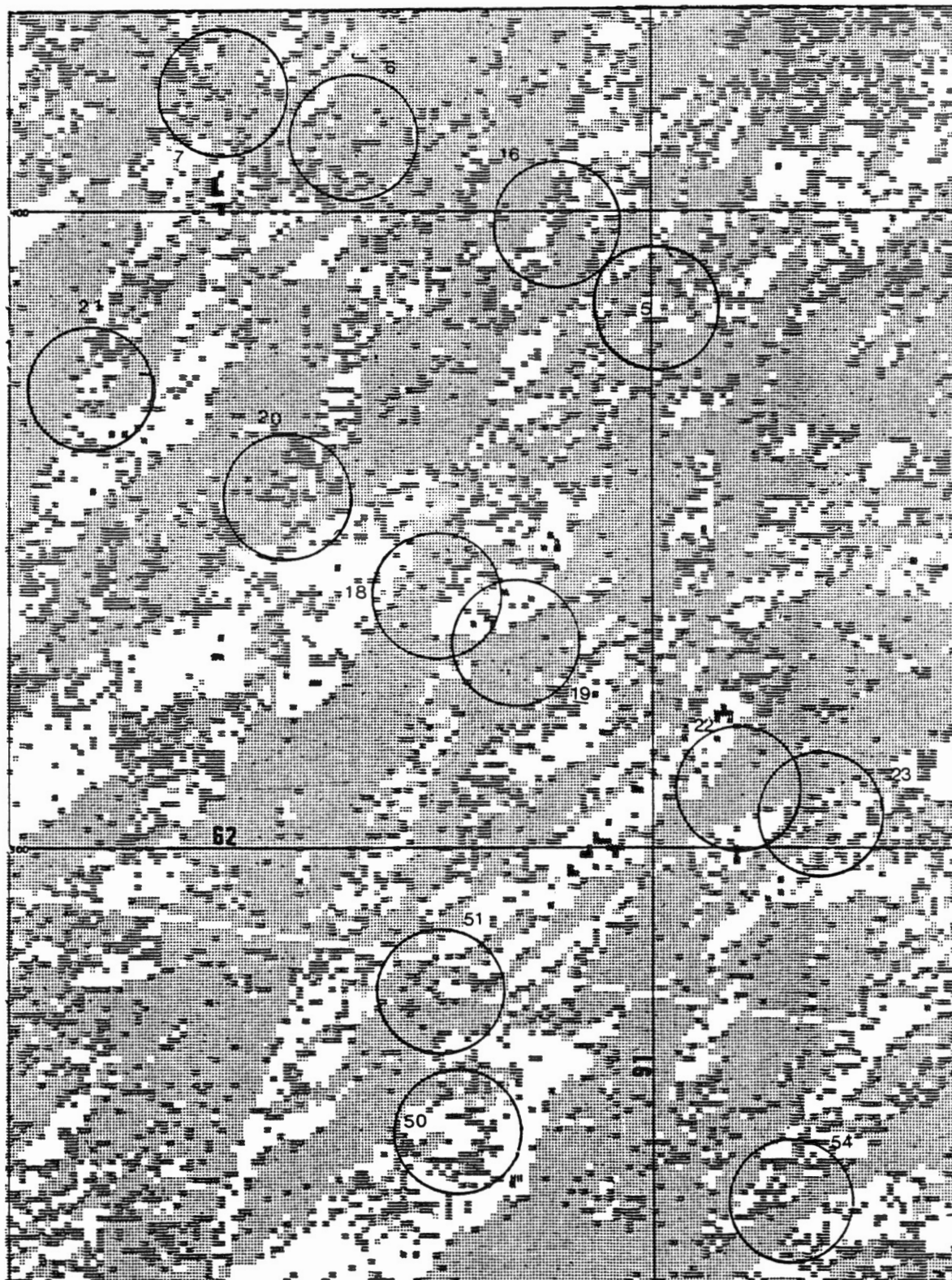


Figure 35. Target 19, Band Ratio Classification, File 2, Scale 1:98, 425

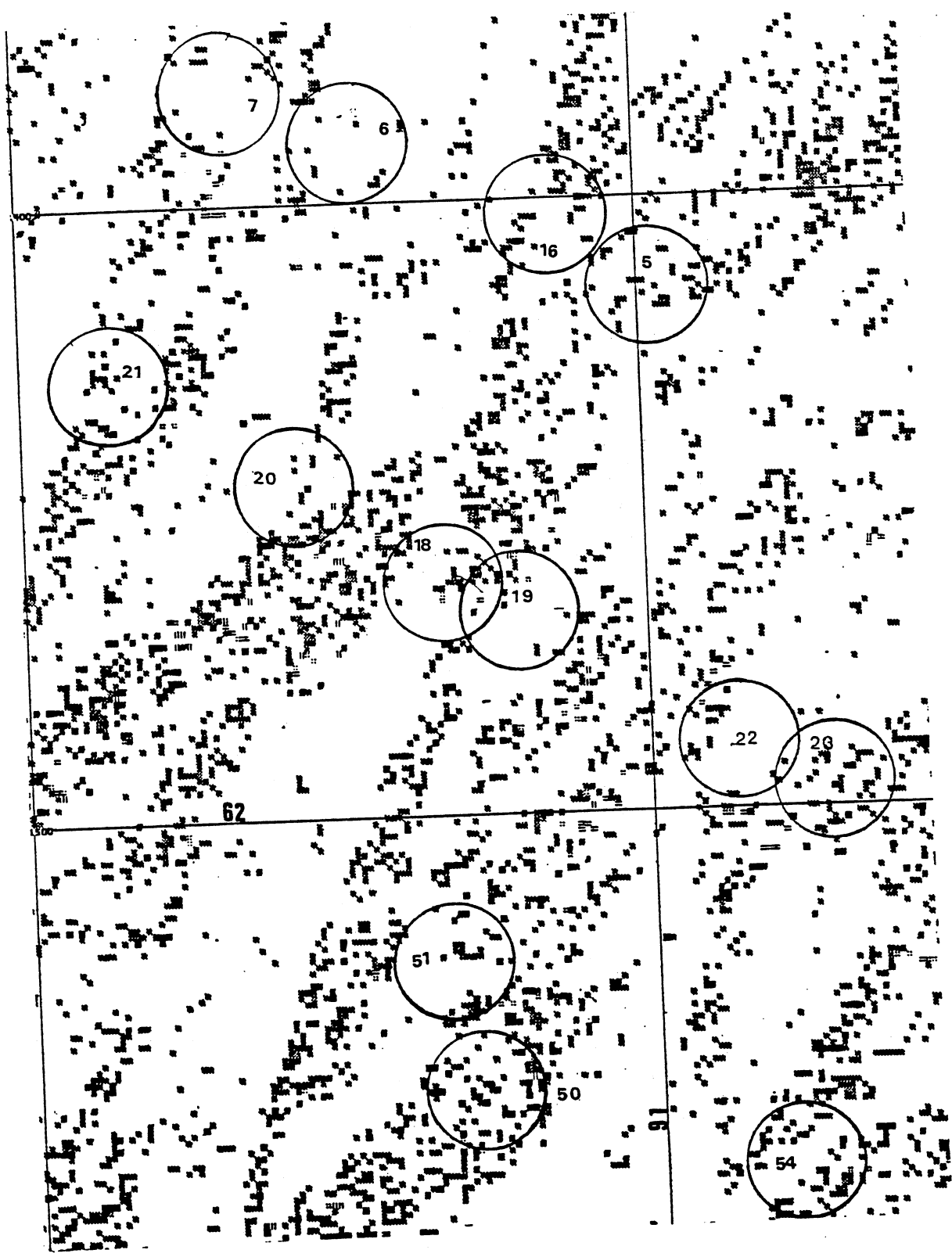


Figure 36. Target 19, Band Ratio Classification, File 3, Scale 1:98, 425

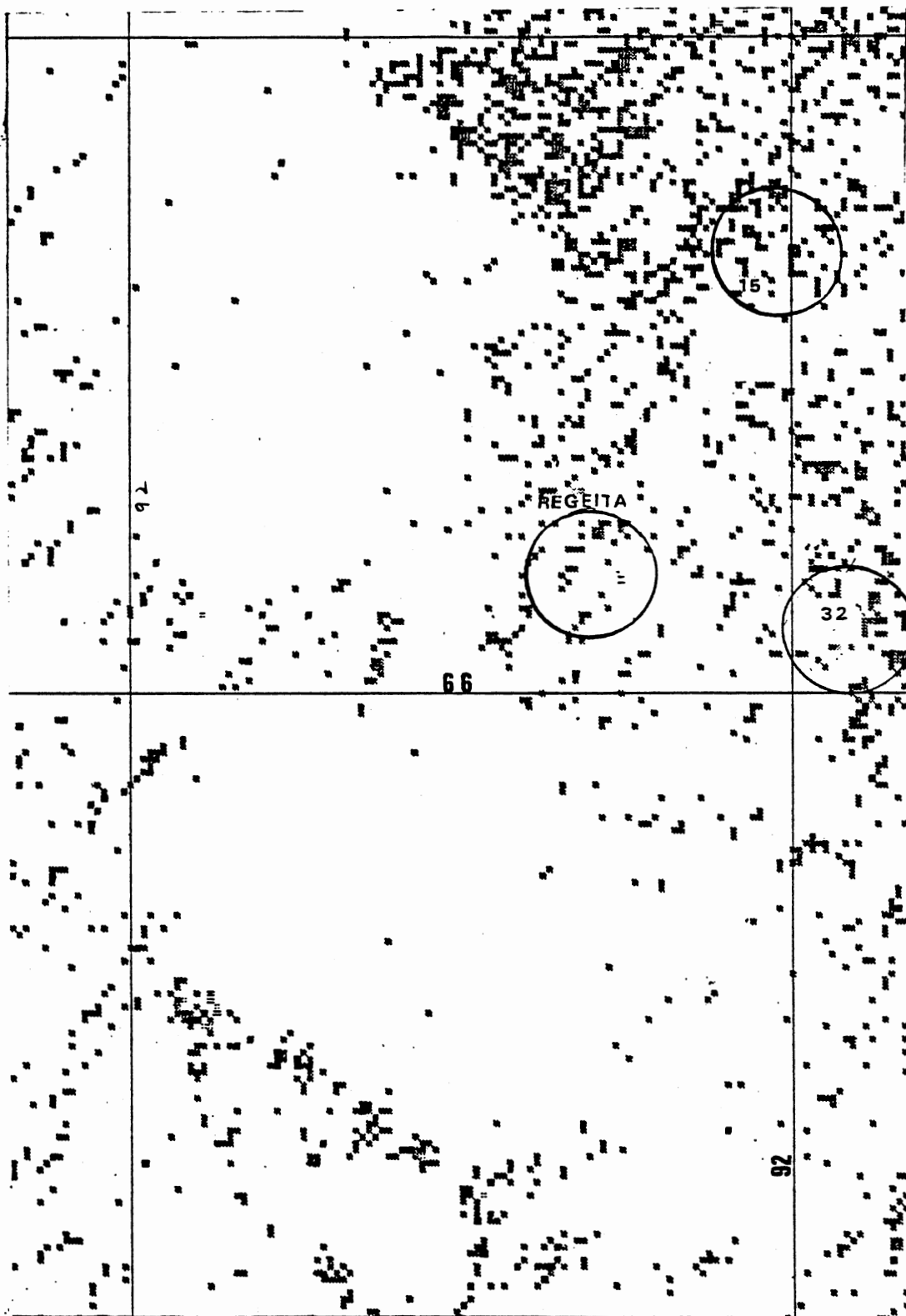


Figure 37. Regeita Area, Band Ratio Classification, Band 1, Scale 1:98, 425

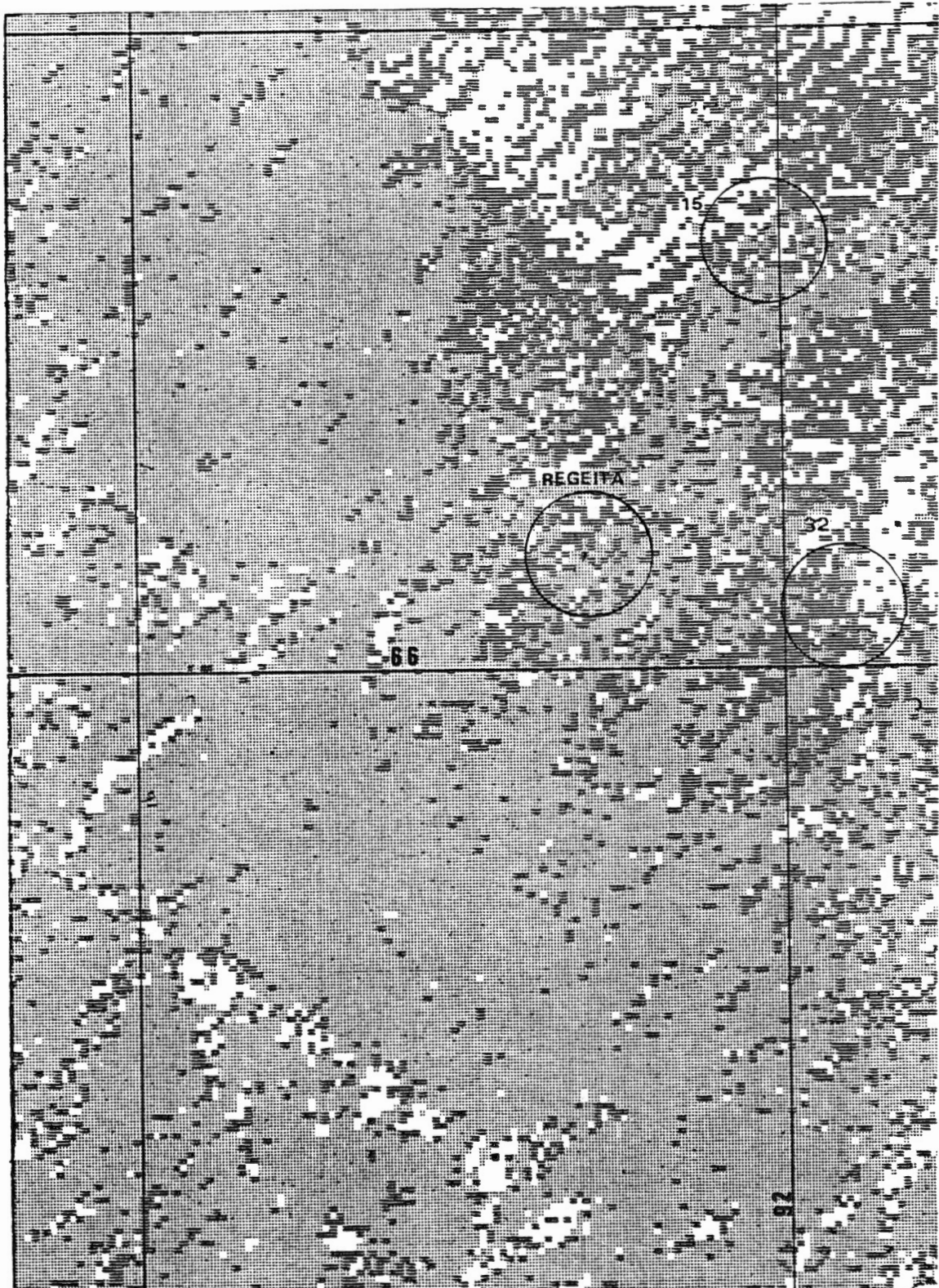


Figure 38. Regeita Area, Band Ratio Classification, Band 2, Scale 1:98, 425

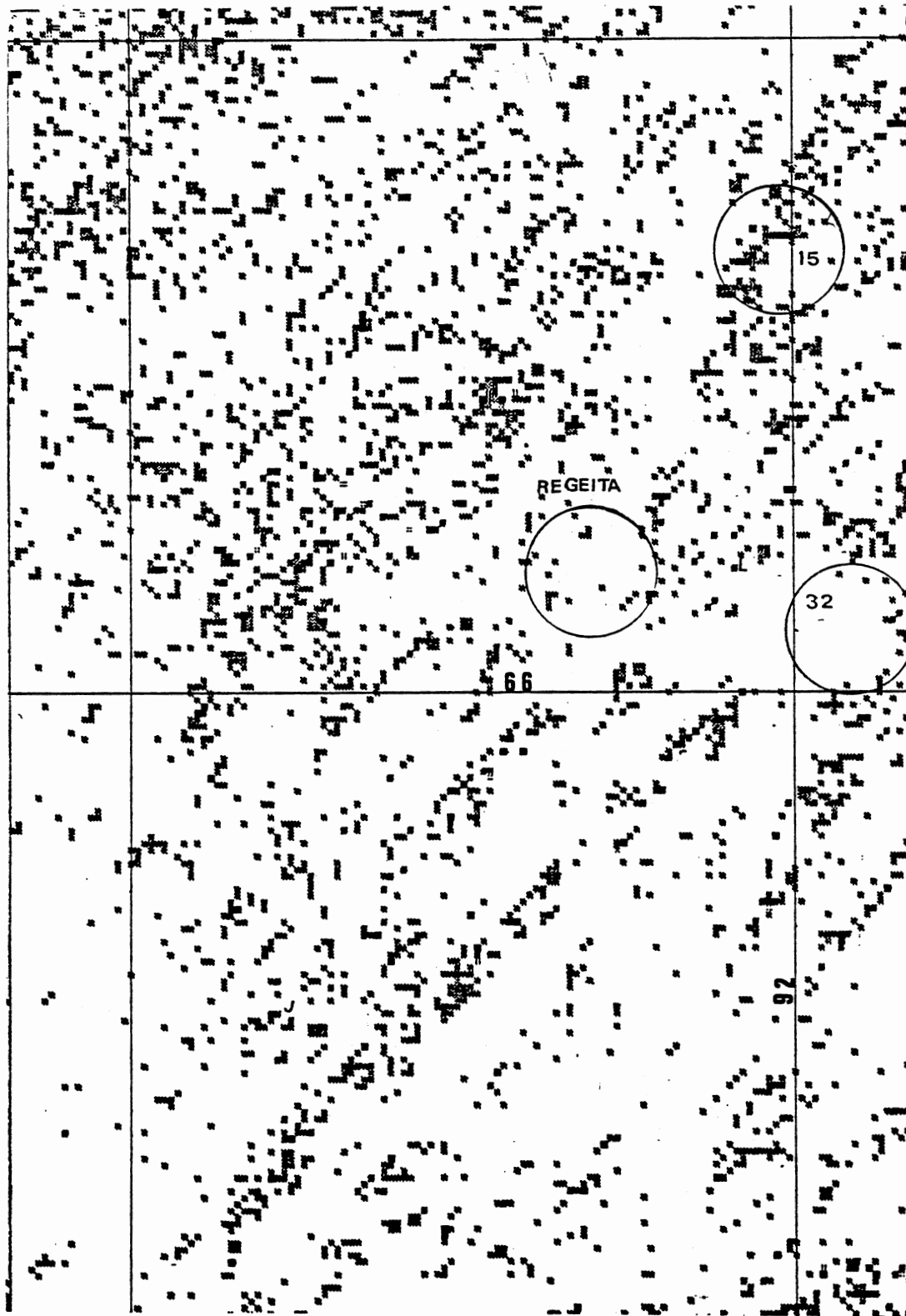


Figure 39. Regeita Area, Band Ratio Classification, Band 3,
Scale 1:98, 425

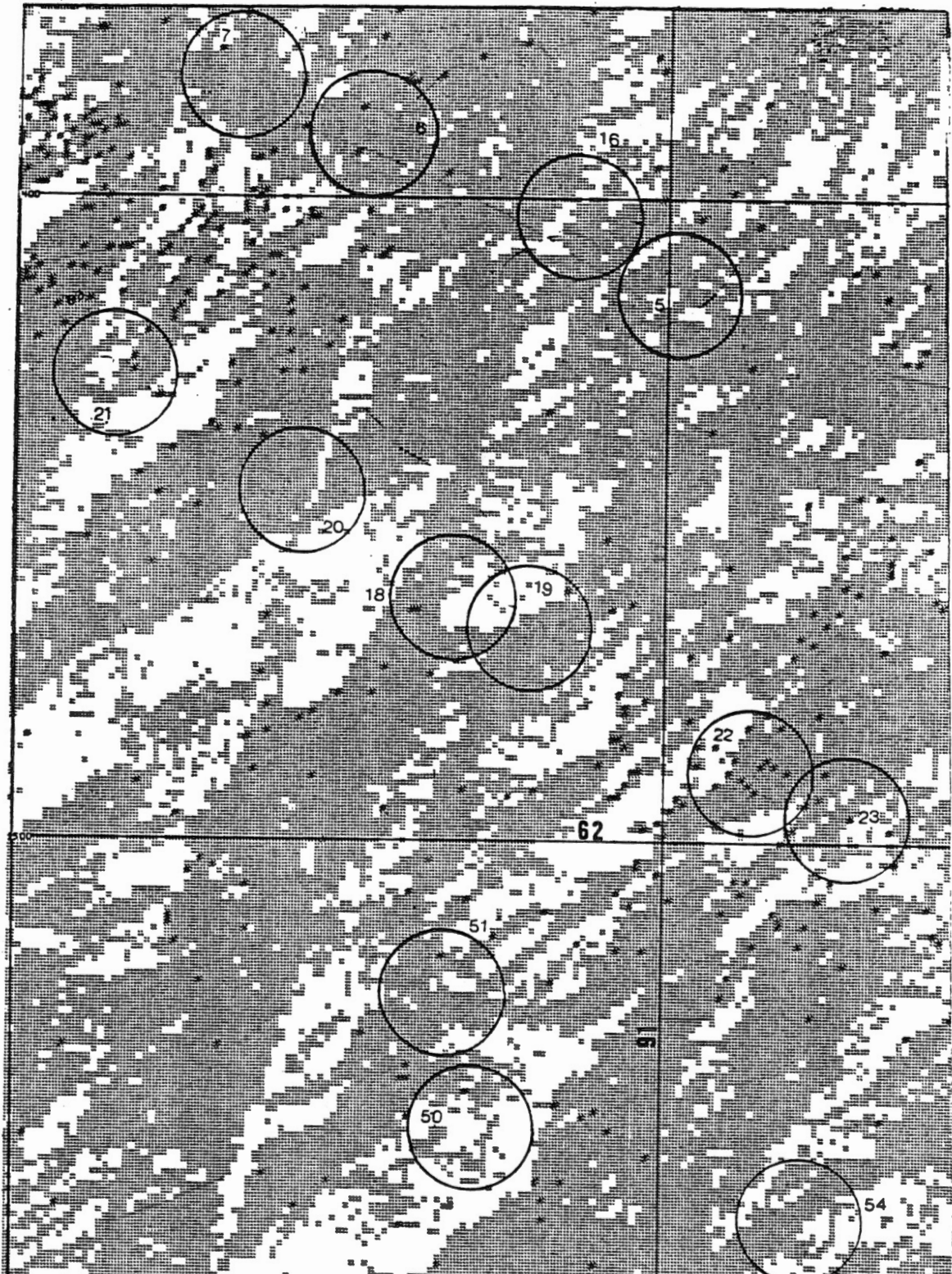


Figure 40. Target 19 Plot Showing Closeness of Match to Altered Rock Spectral Reflectance Values, Using Band Ratio Data.
 Black = 3 Ratios Match, Diagonal = 2 Match, Dot = 1 Match

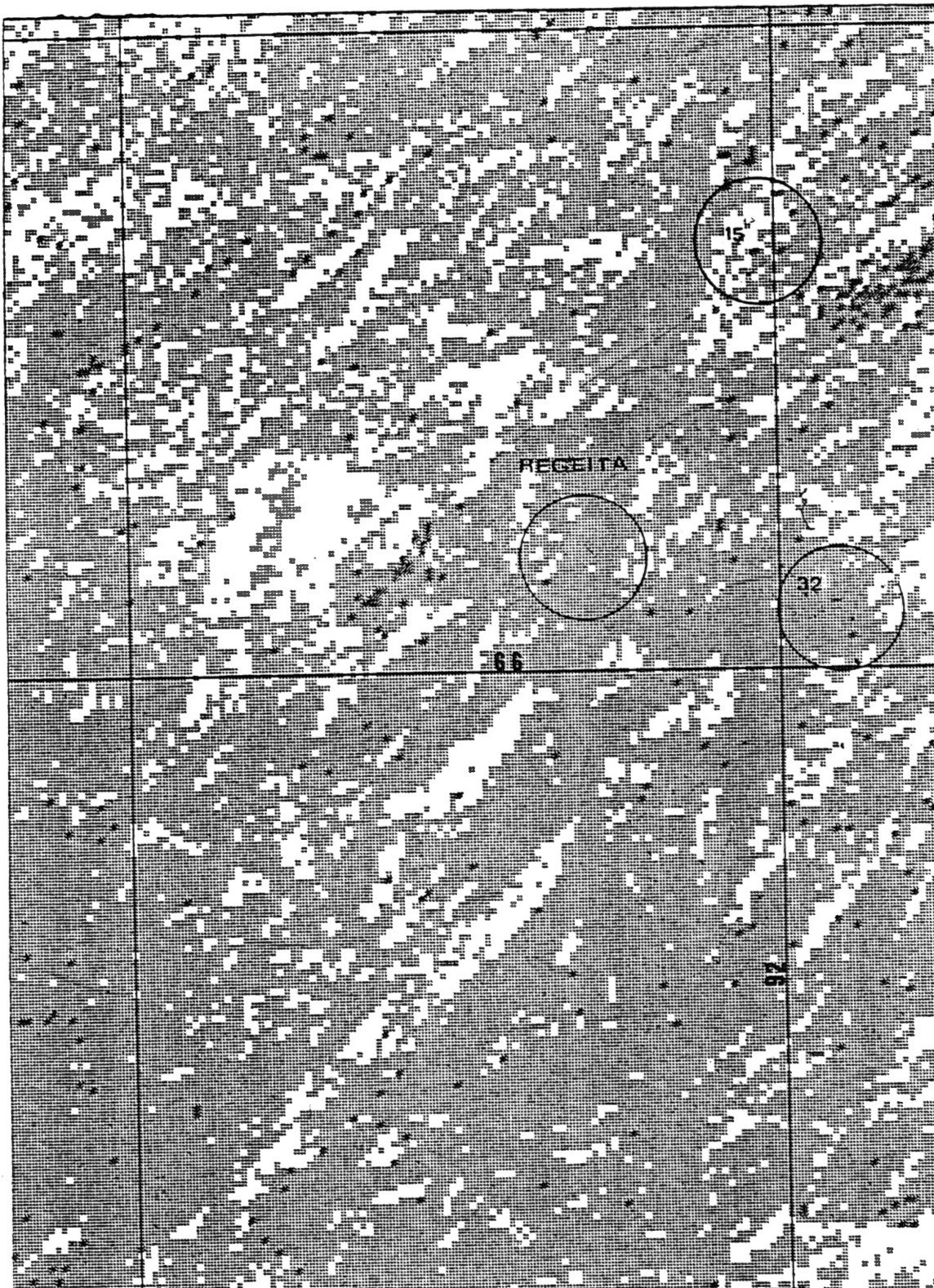


Figure 41. Regeita Area Plot Showing Closeness of Match to Altered Rock Spectral Reflectance Values, Using Band Ratio Data. Black = 3 Ratios Match, Diagonal = 2 Match, Dot = 1 Match

APPENDIX C

EXCERPTS FROM ROAD LOG

Introduction

The writer, accompanied by Dr. Raafat Misah of the Desert Institute of Egypt, made field studies of the copper deposits and of the associated igneous and metamorphic rocks; the studies were undertaken January 12-17, 1982. The excerpts below are from the field notes written during that time.

Unless otherwise stated, all rock units are Precambrian in age.

Wadi Sidr Region

Km 573: Junction with Abu Zenima - El Tor Road. Head E into Wadi Sidr.

Km 596: Nubian sandstone, probably carboniferous, on north side of wadi. Red granite on south side. Sandstone is very ferruginous, dark red. Granite has quartz veins. Joints in the granite trend $N72^{\circ}E$ and $N53^{\circ}W$.

Km 598: Vertical basalt dike is exposed on north side of wadi. Fractures in basalt trend $N27^{\circ}E$.

Wadi Sahab Region

Km 549: Turn south into Wadi Sahab at El Sahab well. Granite outcrop at this spot is a gray granite with pink orthoclase phenocrysts and with biotite. Veins 8 inches thick of dark red granite have been epidotized. Phenocrysts of orthoclase in host granite are larger near the veins.

Km 854: Basalt dike; the basalt is red-brown in color.

Km 857: A very large, very weathered dike is present at this

locality; probably Miocene in age and very basic in composition--possibly dunite.

Km 867: Abu Suweita. School building at this location. We are now out of Wadi Sahab. A small oasis is exposed in the wadi below the school. At this point a dike blocks water flow beneath the wadi surface. This can be seen in the photograph (Figure 42).

Regeita

The main fault strikes $N53^{\circ}W$; dips 78° to the SW. The breccia zone within the fault averages 5 feet wide, but in places is 10 feet wide. Excavations in the fault are as deep as 30 feet and still show mineralization. No visible alteration. Blue (chrysocolla?) and green (malachite) minerals on walls of fault and on pieces of fault breccia. Aphaartic dike (basalt?) strikes $N38^{\circ}E$; dip is vertical.

All mineralization is topographically above and north of the dike. Other faults nearby are not mineralized. No sulfides can be seen. Blue mineral is sometimes botryoidal.

El Tarr

(See Figures 13-17). Blue to blue-green mineralization in granite is intruded into schist. Fractures, trending $N27^{\circ}E$, in granite, are heavily stained by the mineral. A brick-red aphanitic dike is 50 meters east of the mineralization, and strikes $N10^{\circ}E$. A wadi is across the Feiran road, and extends $N30^{\circ}E$. A bluff to the east of that wadi contains a near-vertical fault. The wadi and the fault, if extended, would



Figure 42. Abu Suweira. Note Palm Trees to Right
of the Dike Cutting Across the Wadi.
D = Dike

intersect in the mineralized area. The mineralized area of the granite appears to be shattered and chaotic.

APPENDIX D

EXPLORATION TARGET LOCATIONS

| Target No. | Universal Trans- verse Mercator Grid (X 10,000) | | Longitude (E) | Latitude (N) |
|---------------|--|-------|---------------|--------------|
| | E | N | | |
| 1 | 92.90 | 67.78 | 34° 13' 9" | 28° 26' 14" |
| 2 | 93.07 | 67.75 | 34° 14' 14" | 28° 25' 57" |
| 3 | 90.90 | 64.00 | 34° 00' 00" | 28° 26' 11" |
| 4 | 90.33 | 66.13 | 33° 58' 27" | 28° 37' 46" |
| 5 | 91.03 | 62.88 | 34° 00' 37" | 28° 19' 55" |
| 6 | 90.55 | 63.10 | 33° 57' 41" | 28° 21' 16" |
| 7 | 90.35 | 63.19 | 33° 54' 53" | 28° 21' 57" |
| 8 | 90.00 | 66.53 | 33° 55' 03" | 28° 39' 49" |
| 9 | 90.03 | 65.80 | 33° 54' 53" | 28° 35' 51" |
| 10 | 89.66 | 66.40 | 33° 52' 44" | 28° 39' 08" |
| 11 | 90.09 | 63.50 | 33° 54' 44" | 28° 23' 35" |
| 12 | 89.83 | 62.95 | 33° 53' 11" | 28° 20' 27" |
| 13 | 91.73 | 64.36 | 34° 05' 15" | 28° 43' 05" |
| 14 | 91.53 | 65.03 | 34° 04' 10" | 28° 31' 30" |
| 15 | 91.98 | 66.68 | 34° 07' 07" | 28° 38' 19" |
| 16 | 90.87 | 62.98 | 33° 59' 50" | 28° 20' 35" |
| 17 | 90.04 | 63.40 | 33° 54' 44" | 28° 22' 54" |
| 18 | 90.68 | 62.40 | 33° 58' 27" | 28° 17' 27" |
| 19 | 90.80 | 62.33 | 33° 59' 13" | 28° 16' 54" |
| 20 | 90.45 | 62.55 | 33° 57' 04" | 28° 18' 16" |
| 21 | 90.15 | 62.73 | 33° 55' 22" | 28° 19' 14" |
| 22 | 91.14 | 62.11 | 34° 01' 23" | 28° 15' 49" |
| 23 | 91.28 | 62.04 | 34° 01' 42" | 28° 15' 24" |
| 24 | 91.46 | 62.95 | 34° 03' 15" | 28° 14' 44" |
| 25 | 91.71 | 61.83 | 34° 03' 52" | 28° 14' 19" |
| 26 | 90.50 | 68.28 | 33° 58' 27" | 28° 53' 10" |
| 27 | 91.02 | 67.90 | 34° 01' 23" | 28° 47' 03" |
| 28 | 91.33 | 67.68 | 34° 03' 10" | 28° 45' 57" |
| 29 | 91.62 | 67.43 | 34° 05' 06" | 28° 44' 27" |
| 30 | 92.71 | 66.00 | 34° 11' 39" | 28° 36' 33" |
| 31 | 92.90 | 65.20 | 34° 12' 32" | 28° 32' 19" |

| Target No. | Universal Trans- verse Mercator Grid (X 10,000) | | Longitude (E) | Latitude (N) |
|---------------|--|-------|---------------|--------------|
| | E | N | | |
| 32 | 92.07 | 66.10 | 34° 16' 01" | 28° 37' 46" |
| 33 | 87.33 | 68.03 | 33° 38' 31" | 28° 48' 16" |
| 34 | 88.00 | 66.58 | 33° 42' 41" | 28° 40' 30" |
| 35 | 87.83 | 66.73 | 33° 41' 36" | 28° 41' 11" |
| 36 | 86.50 | 69.08 | 33° 31' 28" | 28° 53' 56" |
| 37 | 87.69 | 66.35 | 33° 40' 30" | 28° 39' 08" |
| 38 | 87.78 | 66.12 | 33° 41' 08" | 28° 37' 59" |
| 39 | 87.85 | 66.02 | 33° 42' 13" | 28° 37' 13" |
| 40 | 88.23 | 67.25 | 33° 44' 04" | 28° 43' 55" |
| 41 | 88.51 | 67.13 | 33° 45' 46" | 28° 43' 22" |
| 42 | 88.40 | 67.30 | 33° 45' 00" | 28° 44' 36" |
| 43 | 88.40 | 57.13 | 33° 45' 00" | 28° 42' 33" |
| 44 | 87.42 | 66.53 | 33° 39' 02" | 28° 40' 01" |
| 45 | 87.53 | 69.26 | 33° 40' 40" | 28° 54' 57" |
| 46 | 90.28 | 65.30 | 33° 56' 31" | 28° 32' 55" |
| 47 | 92.55 | 62.67 | 34° 10' 40" | 28° 18' 41" |
| 48 | 92.28 | 62.14 | 34° 08' 21" | 28° 15' 45" |
| 49 | 92.10 | 62.00 | 34° 07' 15" | 28° 15' 0" |
| 50 | 90.72 | 61.57 | 33° 58' 32" | 28° 12' 57" |
| 51 | 90.70 | 61.72 | 33° 58' 27" | 28° 13' 46" |
| 52 | 90.87 | 61.17 | 33° 59' 0" | 28° 10' 50" |
| 53 | 91.23 | 61.43 | 34° 01' 42" | 28° 12' 12" |
| 54 | 91.75 | 61.16 | 34° 04' 48" | 28° 10' 30" |
| 55 | 90.32 | 63.52 | 33° 56' 28" | 28° 24' 16" |
| 56 | 91.30 | 64.38 | 34° 02' 47" | 28° 27' 57" |
| 57 | 91.61 | 64.00 | 34° 04' 11" | 28° 25' 56" |
| 58 | 91.45 | 64.02 | 34° 03' 19" | 28° 26' 11" |

VITA

Kenneth Elmus Quinn

Candidate for the Degree of

Master of Science

Thesis: SELECTION OF POTENTIAL MINERAL DEPOSITS IN SOUTHWESTERN SINAI
USING LANDSAT IMAGES

Major Field: Geology

Biographical:

Personal Data: Born in Gadsden, Alabama, February 10, 1947, the
son of Elmus and Anne Quinn.

Education: Graduated from Etowah County High School, Attalla, Ala-
bama, in May, 1965; received Bachelor of Science degree in
Geology from the University of Alabama in 1970; enrolled in
Master's program in geology at the University of Nebraska,
1972; received Master of Library Science degree from the Uni-
versity of Alabama, 1974; completed requirements for the Mas-
ter of Science degree at Oklahoma State University in July,
1983.

Professional Experience: Paleontologist, University of Nebraska
State Museum, 1970-1972; geologist and librarian, Arkansas
Geological Commission, 1974-1977; Assistant librarian, Okla-
homa State University, 1977-1979; Management services analyst,
Phillips Petroleum Company, 1979-1980; graduate teaching
assistant, Oklahoma State University, Department of Geology,
1980-1982; Librarian of Bartlesville Energy Technology Center,
1982.